Clinical and Genetic Analysis of Alopecia and Ectodermal Dysplasia in Three Consanguineous Families

by

Fatima Ansar Abbasi

Department of Biochemistry
Faculty of Biological Sciences
Quaid-i-Azam University
Islamabad, Pakistan

2021

Clinical and Genetic Analysis of Alopecia and Ectodermal Dysplasia in Three Consanguineous Families

A thesis submitted in the partial fulfillment of the

requirements for the degree of

Master of Philosophy

In

Biochemistry/Molecular Biology

by

Fatima Ansar Abbasi

Department of Biochemistry
Faculty of Biological Sciences
Quaid-i-Azam University
Islamabad, Pakistan
2021

DEDICATED

TO

MY LATE FATHER AND

FAMILY

FOR THEIR ENDLESS LOVE,

SUPPORT,

ENCOURAGEMENT AND

PRAYERS!

In the Name of ALLAH, the Most Gracious, the Most Merciful.

CERTIFICATE

This thesis, submitted by **Ms. Fatima Ansar Abbasi** to the Department of Biochemistry, Faculty of Biological Sciences, Quaid-i-Azam University, Islamabad, Pakistan, is accepted in its present form as satisfying the thesis requirement for the Degree of Master of Philosophy in Biochemistry/Molecular Biology.

Supervisor:

Dr. Wasim Ahmad
Professor

External Examinar:

Dr. Muhammad Jawad Hassan
Associate Professor
National University of Medical Sciences
The Mall Road, Rawalpindi.

Chairperson:

Dr. Iram Murtaza
Professor

Dated: November 23, 2021

Declaration

I hereby declared that the work presented in this thesis is my own effort and hard work and it is written and composed by me. No part of this thesis has been previously published or presented for any other degree or certificate.

Fatima Ansar Abbasi

Table of Contents

Acknowledgements I

List of Figures III

List of Tables VII

List of Abbreviations VIII

Abstract XIV

Introduction 1

Ectodermal Appendages 1

Nail 1

Teeth 1

Sweat Glands 2

Hair 2

Hair Structure and Formation 2

Hair follicle 3

Hair Follicle Cycle 4

Hair Functions 4

Hair Morphogenesis 4

Molecular Pathways in Hair Morphogenesis 5

Hair Loss Disorders/Alopecia 5

Congenital Alopecia 6

Loose Anagen Hair Syndrome 6

Short Anagen Syndrome 6

Aplasia Cutis Congenital 6

Congenital Triangular Alopecia 7

Congenital Atrichia 7

Congenital Hypotrichosis 7

Hereditary Hypotrichosis Simplex Type 1 8

Hereditary Hypotrichosis Scalp Type 2 8

Hereditary Hypotrichosis 3 and Wooly Hair 8

Hypotrichosis 4 Marie Unna Hereditary Hypotrichosis 1 (MUHH1) 9

Hypotrichosis 5 (MUHH2) 9

Hereditary Hypotrichosis Simplex 3 (HSS3/HYPT11) 9

Hereditary Hypotrichosis Simplex 4 10

Atrichia with Papular Lesions (APL) 10

Localized Autosomal Recessive Hypotrichosis 1 10

Localized Autosomal Recessive Hypotrichosis 2 11

Localized Autosomal Recessive Hypotrichosis (LAH3) 11

Autosomal Recessive Hypotrichosis 9 12

Autosomal Recessive Hypotrichosis 10 12

Hypotrichosis with Recurrent Skin Vesicle 12

Digenic Autosomal Recessive Hypotrichosis 12

Acquired Alopecia 13

Syndromic Forms of Alopecia 14

Hypotrichosis with Cone-Rod Dystrophy (HJMD) 14

Alopecia and Mental Retardation Syndrome 14

Woodhouse Sakati Syndrome 14

Ectodermal Dysplasias (ED) 15

Palmoplantar Keratoderma 15

Diffuse Palmoplantar Keratoderma (DPPK) 16

Diffuse PPK without Transgrediens 16

Diffuse PPK with Transgrediens 16

Focal Palmoplantar Keratoderma 17

Striate Palmoplantar Hyperkeratosis 17

Punctate Palmoplantar Keratoderma 18

Materials and methods 21

Study Subjects 21

Pedigrees/Family Charts 21

Collecting Blood Specimens 21

Genomic DNA Extraction 22

DNA Extraction by Phenol-Chloroform Method 22

DNA Extraction Using Commercially Available Kit Procedure 24

Agarose Gel Electrophoresis (1%) 25

DNA Quantification 26

Genotyping and Linkage Analysis/Homozygosity Mapping 26

PCR Amplification 27

Polyacrylamide Gel Electrophoresis (PAGE) 27

Sanger Sequencing of Genomic DNA 28

First Sequencing PCR or Pre-sequencing PCR including 28

First Purification of Amplified PCR products 29

Primer Designing 29

Analysis of Sequencing Data and Variant Validation 30

Results 34

Recruitment of Families 34

Family A 34

Family B.....34

Family C.....35

Mapping Candidate Genes Involved in Causing Alopecia and Ectodermal.....35

Sequencing Candidate Genes in Family B and C.....37

Discussion.....59

References.....64

ACKNOWLEDGEMENTS

All praises and glories to **Almighty "ALLAH"** who says in the Holy Quran, "And your Lord is the most gracious who taught by the pen. Taught man (those things) which he did not know". Countless Darood on the Prophet **HAZRAT MUHAMMAD (Sall-Allah-Ho-Alaihay-Wa-Aalayhi-Wasallam),** who showed the path of knowledge to the mankind and gave the lessons of seeking knowledge from cradle to the grave. I am greatly honored to pay my deep gratitude to my most learned, perfectionist and considerate supervisor **Prof. Emeritus. Dr. Wasim Ahmad**, Department of Biochemistry, Faculty of Biological Sciences, Quaid-I-Azam University Islamabad, under whose inspiring guidance, valuable suggestions, immense patience and encouragements this research work was carried out. Without his support and kind efforts this task would have been impossible. I'm thankful to Ex-Chairperson, Department of Biochemistry, **Dr. Rashid Khan** for his dedication to facilitate the research activities in the department. I want to express my gratitude to **Dr. Imran Ullah** to help us thrive the research activities in the laboratory. I wish to express sincere thanks to my worthy seniors **Mr. Bilal Khan, Mr. Abdullah, Ms. Rubab Raza, Ms. Hajra Fayyaz, Dr. Shabbir** for their cooperation, suggestions and nice company during my research work, which is precious to me in all regards. I would like to specially acknowledge **Mr. Hammal Khan Zehri and Dr. Muhammad Shoaib Nawaz Khattak,** especially, because without their help and cooperation in my research, though not impossible, but would be really difficult. I acknowledge the friendly and cooperative attitude of my lab fellows: **Rabiha Mushtaq, Shah Hussain, Mariam Jahan, Anam Seemab, Amir Sohail, Bashir Ahmad, Ajmal Safi and Tahir.** I present heartiest thanks to my dear friends **Zohra Jabeen, Maryam Ashraf, Mehreen Tariq, Faiza Zafar, Wajeeha Waheed, Tatheer Zehra and Kaveeta Kumary,** for their constant support and prayers throughout my research. I want to extend my deepest thanks to all the **research volunteers** who participated in the study and gave their consent that aided us conduct the research smoothly.

Special thanks to my teachers who have always been very supportive and have instilled in me the sense of hard work, determination and consistency including **Dr. Asma Gul,**

Dr. Bashir Ahmed, Dr. Bushra Hafeez kiani, Dr Fareeha Jabeen and Dr. Shaheen Shahzad. Much appreciation to **Fareeha Khalid Ghori, Amna Tahir, Sannia Batool, Attiya Zainab, Huma Maqbool, Mafaza Nasim, Shanze' Malik, Rafia Qureshi, Hiba Riaz, Zarah Javed and Naira Rahim Khan** because they filled every moment of my life with such joy that I never felt any moment of sadness. Time spent with them can never be erased from my memories. No words can express my deepest gratitude and feelings to my dearest father **Ansar Ahmed Abbasi (LATE)** and **mother**, whose firm dedication, in-built confidence and untiring efforts have adorned me with the jewels of education. I also owe deepest gratitude to my sisters **Saba Ansar Abbasi, Sadaf Ansar Abbasi, Amna Ansar Abbasi and Hajra Ansar Abbasi** for their moral support, love and prayers throughout my studies which helped to complete my research work. May they be included among those whom Allah loves the most, Ameen. At last but not the least, I convey my heartiest thanks to the departmental clerical staff especially **Mr. Tariq, Mr. Fayyaz** and **Mr. Shehzad,** for their services towards students.

Fatima Ansar Abbasi

List of Figures

Figure No	Title	P. No
1.1	Structure of human hair	3
3.1	Pedigree of family A, segregating a non-syndromic form of alopecia. Circles indicate females and squares represent males. Affected members are denoted by shaded symbols whereas, unaffected members with the unshaded symbols Roman numerals reveal the generation number of individuals within a pedigree while Arabic numerals show the position of members within a generation. Asterisk (*) labeled shapes indicate the members whose blood is drawn	38
3.2	Affected individual (III-3) of family A displaying non-syndromic form of congenital alopecia. Images show sparse body hair (C) especially of the scalp (B), with absent eyebrows and eyelashes. Beard is also absent. Triangular shaped face is also seen in the above image (A). No other associated abnormalities were reported. Pictures were taken and presented here with the consent of the elders of family.	38
3.3	Pedigree chart of family B segregating a syndromic form of alopecia. Males are shown by squares while females by circles. Completely filled shapes illustrate the members with hypotrichosis while the unfilled ones represent the normal individuals. Double lines highlight the consanguineous unions. Roman and the Arabic numerals are used to represent the generation number and the members in the pedigree, respectively. Shapes with the asterisk (*) symbolize the members from whom the blood was collected.	39
3.4	Affected individuals of the family B (III-7, III-9 IV-7, IV-9) displaying a syndromic form of alopecia. Images show that the patients have sparse wooly hair on the scalp (A). Eyelashes, eyebrows, and beard hair are also sparse (B, C). Hypodontia (C) and nail discoloration are also seen in the above pictures (D).	40
3.5	Pedigree sketch of family C with syndromic form of palmoplantar keratoderma having autosomal recessive pattern of Mendelian inheritance. Normal members are represented using the colorless symbols while affected members are symbolized by colored shapes. Double lines show the cousin marriages. The asterisk (*) marked individuals show the samples that are available for the study.	41

3.6	Affected individuals of the family B (III-6, IV-1, IV-2, IV-3) with clinical features of palmoplantar keratoderma (E). Diffuse PPK with trans-gradients showing hyperkeratotic plaques on ankles, knees, palms, and the soles surface are seen in the pictures (A, B, C). Hammertoes and chipped tooth phenotypes are also shown by the patients (D).	42
3.7	The Electropherogram shows the allelic pattern of family A amplified using microsatellite markers flanking the *LIPH* gene on chromosome 3q27.2. Here, Lane 1 and 2 shows results for normal individuals (II-1and 2-II-2 while Lane 3 shows results for affected individuals (III-3). In the pedigree, Arabic numbers represent the postions of the individuals within a generation and Roman numerals specify the individual's number within the generation.	43
3.8	The Electropherogram shows the allelic pattern of family A amplified using microsatellite markers flanking the *HR* gene on chromosome 8p21.3. Here, Lane 1 and 2 shows results for normal individuals (II-1and 2-II-2 while Lane 3 shows results for affected individuals (III-3). In the pedigree, Arabic numbers represent the postions of the individuals within a generation and Roman numerals specify the individual's number within the generation	44
3.9	The Electropherogram shows the allelic pattern of family A amplified using microsatellite markers flanking the *LPAR6* gene on chromosome 13q14.2. Here, Lane 1 and 2 shows results for normal individuals (II-1and 2-II-2 while Lane 3 shows results for affected individuals (III-3). In the pedigree, Arabic numbers represent the postions of the individuals within a generation and Roman numerals specify the individual's number within the generation.	45
3.10	The Electropherogram shows the allelic pattern of family A amplified using microsatellite markers flanking the *DSG4/DSC3* gene on chromosome 18q21.1. Here, Lane 1 and 2 shows results for normal individuals (II-1and 2-II-2 while Lane 3 shows results for affected individuals (III-3). In the pedigree, Arabic numbers represent the postions of the individuals within a generation and Roman numerals specify the individual's number within the generation.	46
3.11	The Electropherogram shows the allelic pattern of family B amplified using microsatellite markers flanking the *HR* gene on chromosome 8p21.3. Here, Lane 1 and 2 shows results for normal individuals (III-10 and III-11) while Lane 3, 4 and 5 shows results for affected individuals (III-7, IV-7, IV-8). In the pedigree, Arabic numbers represent the postions of the individuals within a generation and Roman numerals specify the individual's number within the generation.	47

3.12	The Electropherogram shows the allelic pattern of family B amplified using microsatellite markers flanking the *DSG4/DSC3* gene on chromosome 18q21.1. Here, Lane 1 and 2 shows results for normal individuals (III-10 and III-11) while Lane 3, 4 and 5 shows results for affected individuals (III-7, IV-7, IV-8). In the pedigree, Arabic numbers represent the postions of the individuals within a generation and Roman numerals specify the individual's number within the generation.	48
3.13	The Electropherogram shows the allelic pattern of family B amplified using microsatellite markers flanking the *LPAR6* gene on chromosome 13q14.2. Here, Lane 1 and 2 shows results for normal individuals (III-10 and III-11) while Lane 3, 4 and 5 shows results for affected individuals (III-7, IV-7, IV-8). In the pedigree, Arabic numbers represent the postions of the individuals within a generation and Roman numerals specify the individual's number within the generation.	49
3.14	The Electropherogram shows the allelic pattern of family B amplified using microsatellite markers flanking the *LIPH* gene on chromosome 3q27.2. Here, Lane 1 and 2 shows results for normal individuals (III-10 and III-11) while Lane 3, 4 and 5 shows results for affected individuals (III-7, IV-7, IV-8). In the pedigree, Arabic numbers represent the postions of the individuals within a generation and Roman numerals specify the individual's number within the generation.	50
3.15	The Electropherogram shows the allelic pattern of family B amplified using microsatellite markers flanking the *CDH3* gene on chromosome 16q21.1. Here, Lane 1 and 2 shows results for normal individuals (III-10 and III-11) while Lane 3, 4 and 5 shows results for affected individuals (III-7, IV-7, IV-8). In the pedigree, Arabic numbers represent the postions of the individuals within a generation and Roman numerals specify the individual's number within the generation.	51
3.16	The Electropherogram shows the allelic pattern of family C amplified using microsatellite markers flanking the *DCAF17* gene on chromosome 2q31.1. Here, Lane 1 and 2 shows results for normal individuals (III-1 and III-4) while Lane 3, 4, 5 and 6 shows results for affected individuals (III-6, IV-1, IV-2, and IV-3). In the pedigree, Arabic numbers represent the postions of the individuals within a generation and Roman numerals specify the individual's number within the generation.	52
3.17	The Electropherogram shows the allelic pattern of family C amplified using microsatellite markers flanking the *SLURP1* gene on chromosome 8q24.3. Here, Lane 1 and 2 shows results for normal individuals (III-1 and III-4) while Lane 3, 4, 5 and 6 shows results for affected individuals (III-6, IV-1, IV-2, and IV-3). In the pedigree, Arabic numbers represent the postions	53

	of the individuals within a generation and Roman numerals specify the individual's number within the generation.	
3.18	The Electropherogram shows the allelic pattern of family C amplified using microsatellite markers flanking the *SDR9C7* gene on chromosome 12q13.3. Here, Lane 1 and 2 shows results for normal individuals (III-1 and III-4) while Lane 3, 4, 5 and 6 shows results for affected individuals (III-6, IV-1, IV-2, and IV-3). In the pedigree, Arabic numbers represent the postions of the individuals within a generation and Roman numerals specify the individual's number within the generation.	54
3,19	The Electropherogram shows the allelic pattern of family C amplified using microsatellite markers flanking the *GJB6* gene on chromosome 13q12.11. Here, Lane 1 and 2 shows results for normal individuals (III-1 and III-4) while Lane 3, 4, 5 and 6 shows results for affected individuals (III-6, IV-1, IV-2, and IV-3). In the pedigree, Arabic numbers represent the postions of the individuals within a generation and Roman numerals specify the individual's number within the generation.	55
3.20	The Electropherogram shows the allelic pattern of family C amplified using microsatellite markers flanking the *NLRP1* gene on chromosome 17q13.2. Here, Lane 1 and 2 shows results for normal individuals (III-1 and III-4) while Lane 3, 4, 5 and 6 shows results for affected individuals (III-6, IV-1, IV-2, and IV-3). In the pedigree, Arabic numbers represent the postions of the individuals within a generation and Roman numerals specify the individual's number within the generation.	56
3.21	The Electropherogram shows the allelic pattern of family C amplified using microsatellite markers flanking the *JUP* gene on chromosome 17q21.2. Here, Lane 1 and 2 shows results for normal individuals (III-1 and III-4) while Lane 3, 4, 5 and 6 shows results for affected individuals (III-6, IV-1, IV-2, and IV-3). In the pedigree, Arabic numbers represent the postions of the individuals within a generation and Roman numerals specify the individual's number within the generation	57
3.22	The Electropherogram shows the allelic pattern of family C amplified using microsatellite markers flanking the *SERPINB7* gene on chromosome 18q21.33. Here, Lane 1 and 2 shows results for normal individuals (III-1 and III-4) while Lane 3, 4, 5 and 6 shows results for affected individuals (III-6, IV-1, IV-2, and IV-3). In the pedigree, Arabic numbers represent the postions of the individuals within a generation and Roman numerals specify the individual's number within the generation.	58

List of Tables

Table No.	Title	Page No.
2.1	Composition of Solutions Used in Genomic DNA Extraction	24
2.2	Composition of Solutions Used in Agarose Gel Preparation	26
2.3	Chemicals Used in PCR master mix	27
2.4	Composition and Concentration of Chemicals Used in Polyacrylamide Gel	28
2.5	List of microsatellite markers used for linkage analysis of candidate gene/loci	31
2.6	List of Primer sequences to PCR-amplify *GJB6*	33
2.7	List of Primer sequences to PCR-amplify *GJA1*	33

List of Abbreviations

%	Percentage
µm	Micrometer
°C	Degree centigrade
AA	Alopecia Areata
Aa	Amino Acids
AAGAB	Alpha and Gamma Adaptin Binding Protein
ACC	Aplasia Cutis Congenital
AD	Autosomal Dominant
AE	Anagen Effluvium
AGA	Androgenetic Alopecia
APCDD1	APC Down-Regulated 1
APL	Atrichia With Papular Lesions
APMR	Alopecia And Mental Retardation Syndrome
APS	Ammonium Persulfate
AQP5	Aquaporin 5
AR	Autosomal Recessive
ARHGAP31	Rho GTPase Activating Protein 31
ARWH	Autosomal Recessive Woolly Hair
BMN	Bone Marrow Necrosis
BMP	Bone Morphogenetic Protein
BMP	Bone Morphogenetic Protein
BMP4	Bone Morphogenetic Protein 4
bp	Base Pair
CA	Congenital Atrichia
CDH3	Cadherin 3
CDSN	Corneodesmosin
CHLD	Congenital Hair Loss Disorders
cM	Centimorgan

CNV	Copy Number Variations
COL14A1	Collagen Type XIV Alpha 1 Chain
CTA	Congenital Triangular Alopecia
C-Terminus	Carboxyl-Terminus
CX30	Connexin 30
CX43	Connexin 43
DCAF17	DDB1 And CUL4 Associated Factor 1
DKK	Dickkopf WNT Signaling Pathway Inhibitor 1
DLE	Discoid Lupus Erythematosus
DLX3	Distal-Less Homeobox 1
DNA	Deoxyribonucleic Acid
dNTPs	Deoxy Nucleotide Triphosphates
DOCK6	Dedicator of Cytokinesis 6
DPPK	Diffuse Palmoplantar Keratoderma
DSC3	Desmocollin 3
DSG1	Desmoglein 1
DSG4	Desmoglein 4
DSP	Desmoplakin
ECTD	Ectodermal Dysplasia
ED	Ectodermal Dysplasia's
EDA	Ectodysplasin-A
EDAR	Ectodysplasin Receptor
EDTA	Ethylene-Diamine- Tetra Acetic Acid
EEM Syndrome	Ectodermal Dysplasia, Ectrodactyly, and Macular Dystrophy Syndrome
EPS8L3	Epidermal Growth Factor Receptor Kinase Substrate 8-Like Protein 3
Et.Br	Ethidium Bromide
F	Forward

FGF4	Fibroblast Growth Factor 4
FLG	Filaggrin
FPK	Focal Palmoplantar Keratoderma
g	Gram
g/mL	Gram Per Milliliter
GJA1	Gap Junction Alpha-1 Protein
GJB2	Gap Junction Beta-2 Protein
GJB6	Gap Junction Beta-6 Protein
GPCRs	G-Protein Coupled Receptors
HED	Hidrotic Ectodermal Dysplasia
HF	Hair Follicle
HH	Hedgehog
HHS1	Hereditary Hypotrichosis Simplex Type 1
HJMD Syndrome	Hypotrichosis With Cone-Rod Dystrophy
HMGL	Human Molecular Genetics Laboratory
HR Gene	Hairless Gene
HRAS	Harvey Rat Sarcoma Virus"
HS	Hair Shaft
HSS3	Hereditary Hypotrichosis Simplex 3
HYPT 1	Hypotrichosis 1
IRB	Institutional Review Board
IRS	Inner Root Sheath
JUP	Junction Plakoglobin
K6HF	Keratin 6 Hair Follicle
kb	Kilo-Base
kDa	Kilodalton
kg	Kilogram
KRT72	Keratin 72
LAH	Localized Autosomal Recessive Hypotrichosis

LAS	Loose Anagen Hair Syndrome
LIPH	Lipase-H
LMX1	LIM Homeobox Transcriotion Factor 1
LPAR6	Lysophosphatidic Acid Receptor 6
M	Molarity
mA	Milliampere
Mb	Mega Base
mg/mL	Milligram Per Milliliter
$Mgcl_2$	Magnesium Chloride
mL	Milliliter
mL/min	Milliliter Per Minute
mm	Millimeter
mM	Millimolar
MSX1	Msh Homeobox 1
MUHH1	Hypotrichosis 4 Marie Unna Hereditary Hypotrichosis 1
MUHH2	Hypotrichosis 4 Marie Unna Hereditary Hypotrichosis 2
NaCl	Sodium Chloride
NAD	Nicotinamide Adenine Dinucleotide
NF-Kb	Nuclear Factor Kappa Light Chain Enhancer Of Activated B Cells
Ng/Ml	Nanogram Per Microliter
NLRP1	NLR Family Pyrin Domain Containing 1
NLS	Nuclear Localization Signal
nm	Nanometer
^oC	Degree Centigrade
OD	Optical Density
p	Short Arm Of Chromosome
PAGE	Polyacrylamide Gel Electrophoresis
PCR	Polymerase Chain Reaction

PDGF	Platelet-Derived Growth Factor
PDGF-A	Platelet-Derived Growth Factor A
PDGFRα	Platelet-Derived Growth Factor Receptor A
pH	Potential of Hydrogen
PK	Proteinase K Enzyme
PPK	Palmoplantar Keratoderma
PPKB	Bothnian PPK
PPK-GN	Gamborg-Nielson PPK
PPKN	Nagashima Type Of PPK
PPKP	Punctate Palmoplantar Keratoderma
PPKS	Striate Palmoplantar Hyperkeratosis
q	Long Arm Of Chromosome
R	Reverse
rpm	Revolutions Per Minute
SAS	Short Anagen Syndrome
SDR9C7	Short Chain Dehydrogenase/Reductase Family 9C Member 7
SDS	Sodium Dodecyl Sulfate
SEM Syndrome	Scalp-Ear-Nipple Syndrome
SERPINB7	Serpin Family B Member 7
SHH	Sonic Hedgehog
SLURP1	Secreted LY6/PLAUR Domain Containing 1
SNRPE	Small Nuclear Ribonucleoprotein Polypeptide E
SPINK5	Serine Peptidase Inhibitor Kazal Type 5
STS	Short Tendem Sequences
TA	Traction Alopecia
Taq	Thermus Aquaticus
TBE	Tris Borateedta
TC	Tinea Capitis
TE	Telogen Effluvium

TE Buffer	Tris- EDTA
TEMED	N, N, N', N'-Tetra Methyl Ethylenediamine
Tfs	Transcription Factors
TKFC	Triokinase And FMN Cyclase
Tm	Annealing Temperature
TNHL	Transient Neonatal Hair Loss
TP63	Tumor Protein P63
TTM	Trichotillomania
UV	Ultraviolet Radiations
v/v	Volume By Volume
WES	Whole-Exome Sequencing
WH	Woolly Hair
WNT	Wingless-Related Integration Site
Wnt7A	Wnt Family Member 7A
WSS	Woodhouse Sakati Syndrome
µg	Microgram
mL	Microliter

Abstract

ABSTRACT

Skin, via its interaction with the external environment, has a protective role along with the distinctive functions of lubrication and thermoregulation. The skin appendages that includes the teeth, nails, hair and sweat glands share common functions like immune surveillance, epidermal barrier, and role in pigmentation and defense mechanism in the skin. Human hair is an utter epitome of aesthetics in our culture. Approximately 5 billion hair are present in humans that act as an outer protective covering. The defects in the expression of the genes that are particularly present in the human hair follicle are associated with the congenital hair loss disorders (CHLD) or Alopecia. Moreover, the phenotypes involving the dry skin, scaling and hyperkeratosis comes under the large group disorders termed as palmoplantar keratoderma (PPK). The molecular characterization of the clinical features underlying PPK have developed a concrete understanding by identifying pathogenic mutations in the genes that have crucial role in skin barrier formation.

The study, presented in the dissertation, potentially investigated the clinical and molecular characterization of three families (A, B, and C) of the Pakistani origin exhibiting consanguineous unions, segregating different types of autosomal recessive congenital hair and ectodermal dysplasia. Family A and B were sampled from Khyber Pakhtunkhwa while family C was sampled from Baluchistan. Family A presented isolated form of alopecia, family B inherited syndromic form of alopecia while family C showed features of PPK with hyperkeratotic plaques on the skin surface of palms, soles ankles, and between the digits. With the aim of establishing the linkage analysis in all the three families, genotyping using the microsatellite markers was performed. The affected individuals present in all the three families were found to be heterozygous for different parental alleles' combinations thus, excluding the families for linkage to pre-existing genes/loci. Furthermore, in the family B and C, Sanger sequencing of single-exon containing genes, *GJB6* and *GJA1*, was performed by dideoxy chain termination method. Analysis of the results failed to show any phenotypic variant, suggesting the involvement of either the regulatory sequences of the genes or another unknown gene present in the same region.

Chapter 1
INTRODUCTION

Introduction

The skin being the largest organ with its characteristic protective role interacts with the external environment along with distinctive functions of thermoregulation and lubrication. The two structural layers of skin; "epidermis" and "dermis" are separated through basal membrane (Chuong *et al.*, 2002). Epidermis being a stratified epithelium has self-renewal, differentiation and proliferation properties (Segre, 2006). It is divided into five layers; stratum corneum, basal layer, upper spinous layer, lower spinous layer, and granular layer (Byrne *et al.*, 2003). The derivation of dermis (corium) from mesoderm makes it a barrier between epidermis and the hypodermis. Different glands, follicles, papillary and reticular layer are the constituents of dermis. The next underlying layer of loose connective tissues and adipose tissues is termed as hypodermis that shows variation in thickness in different body parts (Clark, 1985).

Ectodermal Appendages

The major skin appendages (teeth, hair, nail, glands) share the unique functions as they act as an epidermal barrier, have role in pigmentation and immune surveillance as well as defense mechanism in the skin (Ross and Christiano, 2006).

Nail

The nail being, a keratinous ectodermal appendage, protects the intricate terminal phalanx (Baran *et al.*, 2012). Nail development is aided by the interlinkage of BMP4, FGF4, Wnt7A and SHH signaling (Chuong *et al.*, 1996). Transcription factors like *LMX1, MSX1* and *Engrailed- 1* also aid in this regard (Chen *et al.*, 1998; Jumlongras *et al.*, 2001).

Teeth

Teeth, parts of craniofacial skeleton, have two main parts: the visible portion being the crown and the anchoring part is the root, which holds them to the jawbone. The mineral component of their assembly is enamel, dentin and cementum (Hu and Simmer, 2007). Signaling pathways i.e. WNT, SHH, BMP, FGF and their transcription factors triggers

the teeth development (TFs) (Tucker and Sharpe, 2004; Sartaj and Sharpe, 2006; Hu and Simmer, 2007; Mikkola, 2007).

Sweat Glands

Tubular and coiled glands that are highly active mini-organs of skin. Homeostatic body temperature is maintained by sweat glands. Shh signaling is involved in sweat gland inititation and subsequent ductal growth. Transcription factors of the Fox family play an important function in controlling sweat glands secretions (Kunisada *et al.*, 2009).

Hair

Humans have approximate 5 million hair (Lai-Cheong and McGrath, 2013) that functions as the protective barrier in the form of the outer covering and is a symbol of aesthetic significance in our culture (McKittrick *et al.*, 2012). Human hair development is compromised in several congenital hair disorders, broadly categorized as Alopecias that can either be isolated or syndromic or occasionally appear with certain other diseased phenotypes. Ectodermal appendages, when defected, rarely overlap with the defects of the hair a condition termed as ectodermal dysplasia. Nonetheless, it is also reported that the defects of hair are shown with unrelated phenotypes (Duverger and Morasso, 2014).

Hair follicle defects underlie a large majority of hair related disorders. It is the region where hair formation and growth initiates. Different layers of the keratinocytes and the trichocytes form hair follicle because of the mesenchymal-epithelial association (Qi and Garza, 2014).

Hair Structure and Formation

Melanin, water, lipids, proteins and a trace amount of elements make up the hair (Harrison and Sinclair, 2003). There are various hair types including the lanugo, vellus, and terminal hair that are seen to be shedding soon after birth, fine hair spread mostly on the body and are long with coarse nature respectively (Lai-Cheong and McGrath, 2017).

The average diameter of a hair fiber is about 50-100 µm (Yu *et al.*, 2017). Epidermally derived hair comprises majorly of two parts i.e. hair follicle which is present in the skin and hair shaft-the visible part seen outside the body (Buffoli *et al.*, 2014). Hair shaft has cross-sectionally following parts: cuticle, cortex, and medulla. Outermost part maintaining mechanical behavior of hair is cuticle. Closely arranged spindle cells, the keratin filaments and the sulphur proteins constitute the cortex that further strengthens the hair is the cortex (Yu *et al.*, 2017). The central portion, consisting of specialized cells with air spaces, is not always necessarily present is the medulla. Only the terminal hair are reported to possess medulla. Previously medulla was found to provide insulation but this role has now been redundant (Harrison and Sinclair, 2003; Lai-Cheong and McGrath, 2017).

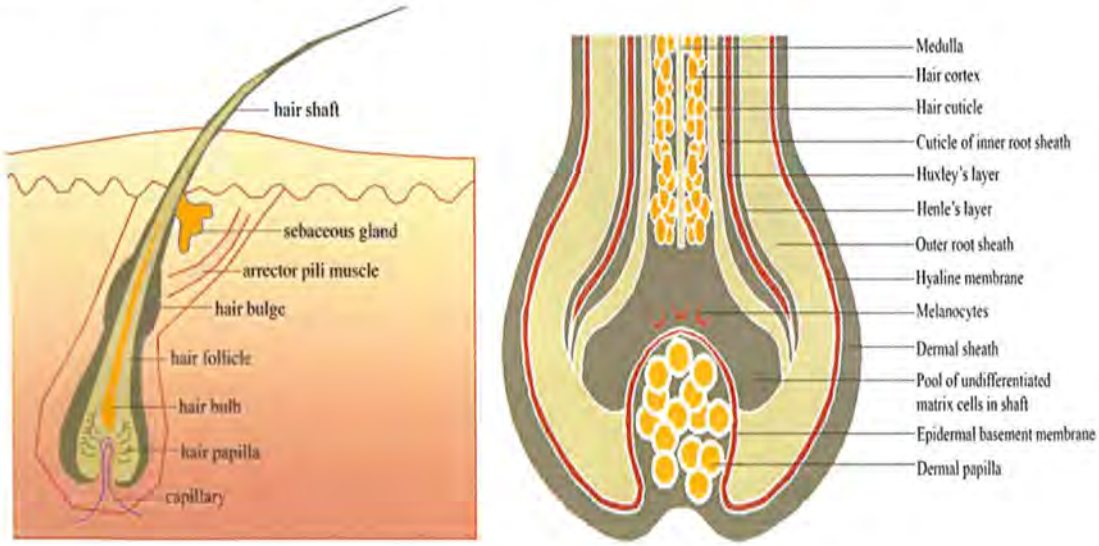

Figure 1: Structure of human hair (Erdoğan, 2017)

Hair follicle

A complex structure (Beigi, 2018) that contains two parts: outer hair root sheath provides protection to growing hair by surrounding hair follicle, and the inner root sheath continues throughout HS till the sebaceous gland opening. Dermal papilla, present at the hair follicle base, is abounded by sensory nerves and also the blood vessels (Gordon *et al.*, 2013). Hair bulb, being the hub of growing hair, is present in the dermal papilla. Hair bulge also resides in hair follicle and has both mesenchymal and epithelial stem cells. Arrector pili muscles are inserted in the hair bulb that upon contraction gives goosebumps (Lai-Cheong and McGrath, 2017).

Hair Follicle Cycle

HF grows dynamically during a normal hair growth cycle (Buffoli *et al.*, 2014) and exhibits three substantial phases namely the anagen, catagen and telogen phase. The longest (about 3-10 years) and the active growth phase is anagen phase. Approximately 84% hair remains in this phase and the hair grows about 1 cm/month (Wolff *et al.*, 2016). The shortest (3-4 weeks) and the growth halt phase is the catagen phase. Approximately only 1% of the hair remain in the growth interruption phase (Qi and Garza, 2014). Hair growth cycle ends with an average length phase (3-4 months) which is the telogen phase where hair loss occurs prior to beginning of a new cycle. About 15% hair stay in the last hair loss phase (Lai-Cheong and McGrath, 2013; Spano and Donovan, 2015).

Hair Functions

Hair is a unique keratinized epidermal derivative that is specifically confined to mammals, mostly spread all over the body except few areas like external genitalia regions, foot sole, palms and lips buccal area. Despite the special and appealing feature in human females, it has a role in skin protection and homeothermy. The androgen-independent hair like eyebrows and eyelashes protect eyes by stopping things from entering them. Head and neck are protected against physical damage, sunlight and severe cold conditions by the scalp hair (Randall and Botchkareva, 2009). Hair also functions in communication be it social or sexual by displaying the sensory function and increasing the skin's perception of various stimuli. Hair have different types on the basis of forms (wavy, straight, and helical), length, diameter, color and cross-sectional shape (Olabiyi *et al.*, 2008; Randall and Botchkareva, 2009; Ito and Wakamatsu, 2011). Hair may be categorized as dead or living depending upon whether it is present inside the skin or outside (Buffoli *et al.*, 2014).

Hair Morphogenesis

During early embryogenesis, the epidermal-dermal junction is the basis for HF morphogenesis having three different stages; induction followed by organogenesis and the last stage is cytodifferentiation (Rishikaysh *et al.*, 2014). In induction phase epidermal thickens and forms hair placode. Next phase is organogenesis that causes the

mesenchymal cells to condensate below the placode. This step forms the basis for the origination of the follicular bud (hair germ). Mesenchymal condensate proliferates with the epithelial cells that invaginate the dermis. Dermal condensate formation is a signal for the hair follicle formation (Yang and Cotsarelis 2010; Welle and Wiener, 2016) and induces dermal papilla formation in the last step of the HF morphogenesis i.e. cytodifferentiation (Welle and Wiener, 2016).

Molecular Pathways in Hair Morphogenesis

The interaction between epithelial and mesenchymal cells by triggering signaling pathways like Wnt or β-catenin, Notch, BMP and hedgehog (HH) pathways are essential for hair follicle development. According to Huang *et al.* (2012), β-catenin/Wnt signaling is the chief regulator of induction phase of HF morphogenesis. Wnt pathway exerts its effects by NF-κB /EDA/EDAR signaling cascade that have hair follicle initiation and primary placode maintenance roles (Biggs and Mikkola 2014). The NF-κB enhances the Shh ligand expression. The sonic hedgehog pathway is involved in morphogenesis and late differentiation. Interaction of laminin-511 and dermal β-1 integrin results in primary cilia formation and enhances the expression of Shh pathway's downstream effectors in dermal lineage. Epithelial PDGF-A association with PDGFRα found on primary cilia also initiates the PDGF signaling. Subsequently, noggin expression is upregulated by dermal Shh and the PDGF signal transduction. Noggin inhibits BMP signaling which blocks β-catenin. Stem cell fate is determined by Notch signaling that is upregulated by the Wnt pathway (Welle and Wiener, 2016). Whereas cellular differentiation is controlled by BMP signaling. Epithelial Shh signaling is upregulated upon communication between dermal and epithelial lineage (Rishikaysh, 2014).

Hair Loss Disorders/Alopecia

The hair follicle expresses a wide range of genes and their underlying defects provide insights for the congenital hair loss disorders (CHLD) or broadly termed as Alopecia particularly in humans. There are approximately 50 CHLD reported which are bifurcated broadly into two forms syndromic or isolated (Shimomura, 2012).

Congenital Alopecia

Loose Anagen Hair Syndrome

Loose Anagen Syndrome (MIM 600628), an autosomal dominant (AD) disorder in which early keratinization of IRS of HF promotes loose attachment of the anagen hair to the HF (Dhurat and Deshpande, 2010; Swink and Castelo-Soccio, 2016; Xu *et al.*, 2017). Individuals with LAS have mutations reported in keratin clusters and the candidate genes include *HRAS* (MIM 190020) *K6HF/KRT75* (MIM 609025), *K6IRS/KRT72* (MIM 608246) and *TKFC* (MIM 615844) (Chapalain *et al.*, 2002; Dhurat and Deshpande, 2010; Onoufriadis *et al.*, 2020) The disease is associated with numerous other congenital abnormalities like coloboma (MIM 120200, 216820), neurofibromatosis-Noonan syndrome (MIM 601321) (Tosti *et al.*, 1991 ; Chapalain *et al.*, 2002).

Short Anagen Syndrome

A hair cycle disorder that prevents long hair growth because the anagen phase is short while telogen phase is longer than usual. Children experience short hair by birth. SAS patients shed hair of almost similar length in the telogen phase as compared to the LAS patients who shed hair of different lengths in the anagen phase. The nature of the SAS is the same as LAS in terms of benign nature and self-limiting growth (Herskovitz *et al.*, 2013). The genetic defects lie in the keratin clusters (Giacomini and Starace, 2011) but the specific genes are yet to be identified. *SPINK5* (MIM 605010) and *DKK1* (MIM 605189) may be associated with the diseased phenotypes. SAS is associated with trichodental dysplasia (MIM 601453) (Kersey, 1987; Avashia *et al.*, 2010) and the genes include *TP63* (603273), *TRPS1* (604386) and *DLX3* (MIM 600525).

Aplasia Cutis Congenital

Aplasia cutis congenital (MIM 107600) is the cutaneous tissue deficiency which mostly includes the scalp. Patients are born with a single lesion on the limbs, trunks or on the scalp with scarring alopecia. Infection, hemorrhage, or thrombosis may occur inside the lesion (Brzezinski *et al.*, 2015). ACC appears in both the forms i.e. isolated as well as the syndromic. Adams-Oliver syndrome (MIM 100300), Wolf-Hirschhorn syndrome

(MIM 194190), Johanson-Blizzard syndrome (MIM 243800), SEN syndrome (MIM 181270) Trisomy 13 are the syndromic forms of ACC (Rodríguez-García *et al.*, 2011) and the genes include *ARHGAP31* (MIM 610911) *BMS1* (MIM 611448), *UBR1* (MIM 605981), *DOCK6* (MIM 614194), *KCTD1* (MIM 181270), *RBPJ* (MIM 147183), *EOGT* (MIM 614789), NOTCH1 (MIM 190198) (Marneros, 2013; Marneros, 2015).

Congenital Triangular Alopecia

A benign non-scarring alopecia previously termed temporal triangular alopecia that shows that the patients exhibit left-sided patches of alopecia that are lancet-shaped, oval, or triangular most frequently involve the frontotemporal scalp (Li *et al.*, 2015). CTA is associated with Trisomy 21 (MIM 190685) and phakomatosis pigmentovascularis. The molecular and the genetic causes of CTA are yet not clear.

Congenital Atrichia

Congenital atrichia (MIM 203655) having AR pattern of inheritance, causes complete loss of hair. Hairless gene (*HR*; MIM 602302) containing 19 exons is mapped on chromosome 8p21-22 (Ahmed *et al.*, 1999) that causes congenital atrichia. The presence of papular lesions on torso region as well as face, neck, scalp and extremities is also presented in patients segregating congenital atrichia. Syndromic forms of congenital atrichia are hidrotic ectodermal dysplasia (MIM 601375) progeria (MIM 176670) and Moynahan syndrome (MIM 203600) (Alves and Grimalt, 2015).

Congenital Hypotrichosis

Hypotrichosis refers to the clinically diverse group of conditions that manifest little to complete hair loss from either scalp region or from the other parts of the body as well. It may be exhibited by the generations either in isolated or syndromic form (Basit *et al.*, 2015).

The types of hypotrichosis that segregate in an autosomal dominant (AD) pattern include:

Hereditary Hypotrichosis Simplex Type 1

HHS1 or HYPT1 (MIM 605389) occurs due to the thinning of scalp hair along with short and sparse body hair. Particularly, the region on the top of head bears lesser hair whereas temples have a bit dense hair. Normal eyelashes, eyebrows and beard are observed (Shimomura *et al.*, 2010). Molecular analysis showed the involvement of 5 exon containing *APCDD1* (MIM 607479) gene spanning a region of 40 kb on chromosomal location 18p11.32-p11.23 (Baumer *et al.*, 2000). Until now only one missense mutation has been reported that changes leucine to arginine (Shimomura *et al.*, 2010; HGMD, 2021). According to uniprot, the membrane tethering protein *APCDD1* contains a signal sequence domain, a transmembrane domain, and a transmembrane helix domain. Further, it is reported to be an inhibitor of Wnt pathway (Shimomura *et al.*, 2010).

Hereditary Hypotrichosis Scalp Type 2

Hereditary Hypotrichosis Scalp Type 2 (OMIM 146520) involves less scalp hair in infants that progresses to adulthood, while the other body hair is normal including eyelashes, eyebrows, and beard. The HYPT 2 causing gene *CDSN* (Corneodesmosin; MIM 602593), comprising 2 exons (Holm *et al.*, 2003) is mapped on chromosome 6p21.3 (Betz *et al.*, 2000). According to HGMD four mutations are associated with *CDSN* gene underlying HYPT2. *CSDN* protein contains N and C terminal glycine loop-related domains and a signal sequence domain (Simon *et al.*, 2001).

Hereditary Hypotrichosis 3 and Wooly Hair

HYPT3 (MIM 194300) characterized by dry, extremely curled, and coarse hair, tapering of the distal ends, twisting, knot formation, dystrophic anagen phase. Chromosomal mapping showed that mutations in *KRT74* gene (MIM 608248), present on chromosome 12q12-q14.1, are associated with HYPT3 (Shimomura *et al.*, 2010). *KRT74* gene consists of 9 exons which encodes 529-amino acid K74 protein having molecular weight of 57.9 kDa. It comprises 3 functional domains including C-terminal tail domain, central domain, and N-terminal head domain (Wasif *et al.*, 2011). To date only three mutations have been identified in *KRT74* associated with Wooly Hair (HGMD).

Hypotrichosis 4 Marie Unna Hereditary Hypotrichosis 1 (MUHH1)

HYPT4/MUHH1 (MIM 146550) involves presence of little hair or loss of complete hair at birth. This AR type of alopecia varies during the individual's developmental stages beginning from coarse hair formation in children to the progressive loss of hair over the years in adults. *HRURF/ U2HR* (MIM 619257), causing HYPT4, resides on chromosome 8p21.2 (van Steensel *et al.*, 1999). According to HGMD, 19 different mutations are identified in the *U2HR* region that led to HYPT4/MUHH1. It is a highly conserved region that encodes a 34 amino acid peptide whose upregulated expression causes enhanced *HR* expression leading to disrupted HF morphogenesis (Wen *et al.*, 2009)

Hypotrichosis 5 (MUHH2)

HYPT5 (OMIM 612841) is the second type of Marie Unna hereditary hypotrichosis. At birth, scalp hair is mostly not present but progressively wire-like and irregular thin hair begin developing in early childhood (Yan *et al.*, 2004). 19 exon containing gene (Tocchetti *et al.*, 2003) *EPS8L3* (MIM 614989), causing HYPT5 was identified using the exome sequencing and is mapped to chromosome 1p21.1-q21.3. To date, only one missense mutation is found in this gene (Zhang *et al.*, 2012; HGMD,2021). *EPS8L3*, belongs to the *EPS8* gene family and contains three domains i.e. SH3 domain, C-terminal effector domain and a PTB (phosphotyrosine binding domain) (Zhang *et al.*, 2012).

Hereditary Hypotrichosis Simplex 3 (HSS3/HYPT11)

Hereditary Hypotrichosis Simplex 3 (MIM 615059) has a variable phenotype primarily beginning with the slight hair thinning at birth and eventually leading to the absent scalp as well as remaining body hair. HYPT 11 causing gene *SNRPE* (MIM 128260), containing 5 exons, was mapped on chromosome 1q31.3-1q41 (Pasternack *et al.*, 2013). HGMD has only 2 repoted mutations in *SNRPE* gene uptil now (HGMD, 2021). *SNRPE* belongs to the Sm protein family that contains a conserved Sm domain present in close proximity of the N-terminal domain. The domain Sm rarely has a variable C-terminal domain present after it (Seraphin, 1995; Salgado-Garrido *et al.*, 1999; Bouveret *et al.*, 2000).

Hereditary Hypotrichosis Simplex 4

Hereditary Hypotrichosis Simplex 4 (MIM 615885) is a phenotype in which the infants, at birth, have a normal scalp hair density. At the age of about 2-6 months, the children suffer progressive hair loss that extends to the complete absence of scalp hair. HYPT12 causing gene *RPL21* (MIM 603636), comprising 6 exons (Yoshihama *et al.*, 2002), mapped to chromosome 13q12.12-12.3 (Xu *et al.*, 2010). Until now single heterozygous mutation is found in the *RPL12* gene (Zhou *et al.*, 2011; HGMD, 2021). The gene belongs to ribosomal protein eL21 protein family and encodes a 160 amino acid containing ribosomal protein-the 60S subunit constituent (Zhou *et al.*, 2011).

The sub-categiries of hypotrichosis that are inherited in an autosomal recessive (AR) manner include:

Atrichia with Papular Lesions (APL)

APL (OMIM 209500) is a phenotype segregated in an either isolated AR pattern (Loewenthal and Prakken, 1961) or a pseudo-dominant pattern (Zlotogorski *et al.*, 2002). In 1999, Kruse *et al.* identified that individuals in the recessive form experience complete hair loss including that of the scalp and whole body and patients also develop keratinous follicular papules. Ahmad *et al.* (1998) mapped the 19 exons containing hairless gene (*HR*; MIM 602302), causing APL, on chromosome 8p21 which was further confirmed by Nothen *et al.* (1998). 52 mutations in *HR* are reported till date (HGMD. 2021). *HR* encodes a protein of 130 kDa with high expression in the HF and acts as a transcription co-repressor for several nuclear receptors. *HR* protein comprises functional domains i.e. a nuclear matrix targeting motif (Djabali *et al.*, 2004), an NLS domain (Djabali *et al.*, 2001), a conserved zinc-finger domain (Ahmad *et al.*, 1998), and a JmjC domain (Clissold *et al.*, 2001).

Localized Autosomal Recessive Hypotrichosis 1

HYPT6 (OMIM 607903) manifests phenotypic variability both intra and inter-familial. Apart from the variable expression, monilethrix (MIM 158000) and HYPT6 are quite similar. The scalp hair may be present or absent at birth or after ritual shaving, may grow again gradually. Normal pubic and axillary hair but scanty to complete absence

of eyebrows, eyelashes. Hair breaks easily as they are thin, flexible, coarse, and brittle (Wajid *et al.*, 2007). Variants in 16 exons containing *DSG4* gene (desmoglein 4; MIM 607892) causing HYPT6 is mapped to chromosome 18q21. To date 8 mutations are reported in *DSG4* underlying HYPT6 (HGMD, 2021). A desmosomal cadherin superfamily member is encoded by *DSG4*. The protein contains various domains; a signal sequence, a propeptide, an extracellular domain with 5 tandem repeats, and a single transmembrane domain (Ullah *et al.*, 2015)

Localized Autosomal Recessive Hypotrichosis 2

HYPT7 (MIM 604379) an AR disorder that phenotypically characterized by scanty wooly scalp hair (Shimomura *et al.*, 2009) displaying thin, almost colorless, and highly curled hair that at a specific point no longer grow. At birth, normal but thin scalp hair may be present that progressively becomes weak and short (Aslam *et al.*, 2004; Jelani *et al.*, 2008). *LIPH* (MIM 607365), being causative gene was mapped on chromosome 3q27.3. To date, in the *LIPH* gene, 25 distinct mutations are identified (HGMD. 2021). *LIPH* comprises 10 exons which encodes a 55kDa membrane associated protein composed of an N-terminal signal sequence and an amino acid triad containing catalytic domain (Sonoda *et al.*, 2002; Aoki *et al.*, 2007).

Localized Autosomal Recessive Hypotrichosis (LAH3)

Wooly hair phenotype also appears in HYPT8 (MIM 278150) in which the patients have curled, lighter color tone and fragile hair that is easily breakable with rare papular lesions confined to occipital area. Body hair including the pubic and axillary hair, eyelashes and eyebrows are normal to scanty (Tariq *et al.*, 2009). The chromosomal location of the gene *LPAR6/P2RY5* underlying HYPT8 was 13q14.11-q21.32 (Wali *et al.*, 2007). To date 25 pathogenic variants in *LPAR6* (MIM 609239) underlying HYPT8 have been reported (HGMD, 2021). The intronic region of the *RB1* gene comprises *LPAR6* gene. *LPAR6* encodes *P2RY5* protein that is a part of purinergic G-protein coupled receptors (GPCRs) family. It is predicted to comprise 7-transmembrane domains, 4 cytoplasmic and 4 extracellular domains (Azeem *et al.*, 2008).

Autosomal Recessive Hypotrichosis 9

The clinical features of the HYPT9 (MIM 614237) were quite similar to the ones observed in individuals underlying other recessive hypotrichosis forms. The HYPT9 was mapped on chromosome 10q11.23-22 (Naz *et al.*, 2010), but the specific gene that segregates the disease is not yet known.

Autosomal Recessive Hypotrichosis 10

The phenotype HYPT10 (MIM 614238) manifests complete hair loss of the scalp along with the presence of papules localized only to the scalp. Mustache and beard are normal or sparse in some cases while eyelashes, eyebrows, and the remaining body hair are less in density and scanty. Using the homozygosity mapping, the disease was mapped on chromosome 7p21.3-p22.3 (Basit *et al.*, 2010), but the specific gene due to which the phenotypes are presented is yet unknown.

Hypotrichosis with Recurrent Skin Vesicle

Hypotrichosis with recurrent skin vesicle (MIM 613102) involves the presence of fragile and thin scalp hair, followed by shedding and then re-growing after ritual shaving. Body hair, axillary hair, eyebrows, and lashes were quite sparse. Scalp and other body regions bear small vesicles that burst, release water and eventually leave a scar. The chromosomal region 18q12.1 is organized in a gene cluster of desmoglein and desmocollin that caused the phenotypes. Sequencing results showed the presence of a mutation in the 16 exon containing *DSC3* gene (MIM 600271) (Ayub *et al.*, 2009). To date only a single mutation is present in *DSC3* gene underlying hypotrichosis with recurrent skin vesicles (HGMD). Similar to other cadherins, *DSC3* protein contains several domains i.e. a signal sequence, a propeptide of 28-125 amino acids, a TM domain, a C-terminal domain and an extracellular domain (Garrod and Chidgey, 2008; Ayub *et al.*, 2009).

Digenic Autosomal Recessive Hypotrichosis

The patients undergoing digenic autosomal recessive hypotrichosis had limited hair growth and either has mild to completely absent hair on the scalp disease-causing genes were mapped on two different chromosomal locations i.e. 12q21.2-q22 and 16q21-

q23.1. Locus on the later chromosomal location was reported to have 16 exon comprising *CDH3* gene (MIM 114021) that has been previously associated with HJMD (OMIM 601553) and EEM syndrome (OMIM 225280) (Basit *et al.*, 2011). Although the retina and macular pigment epithelium of the patients are normal yet they presented certain mutations in the *CDH3* gene that truncated the protein. It was concluded that a phenotype modifier loci mapped on 12q21.2-q22 chromosomal location explicitly showed a combined mutational effect with the first loci to produce the diseased phenotype (Basit *et al.*, 2015). To date, 28 mutations are present in the *CDH3* gene underlying the digenic autosomal recessive hypotrichosis (HGMD). *CDH3* protein has 5 extracellular domains, a TM domain and an intracellular tail region (Jelani *et al.*, 2009).

Acquired Alopecia

Several forms of alopecia are acquired, yet some of them do have unknown genetic causes. Tinea capitis is an infection-based hair loss that have scaling, erythema with or without scarring (Zaraa *et al.*, 2013; Castelo-Soccio, 2014; Fremerey *et al.*, 2018). Persons with autoimmune disorders develop alopecia areata and experience hair loss in round patches that may be asymptomatic or sometimes nail pitting is observed (Safavi, 1992; Alkhalifah *et al.*, 2010). Compromised health conditions medications, metabolic instabilities, and nutritional insufficiencies may develop telogen effluvium, a spontaneous change from anagen to telogen phase causing hair thinning and ultimate shedding (Headington, 1993; Castelo-Soccio, 2014; Alves and Grimalt, 2015). Chemo/radiotherapy, autoimmune disorder, malnutrition, toxins exposure, or infections may develop anagen effluvium, hair shedding during anagen phase occurs causing a type of diffuse non-scarring alopecia (Kanwar and Narang, 2013; Cotter *et al.*, 2017).

Trichotillomania (MIM 613229) is caused when hair is subjected to repetitive pulling followed by distress (Lewin *et al.*, 2009; Alves and Grimalt, 2015; Grant and Chamberlain, 2016). It may have genetic basis and the gene underlying the disorder is *SLITRK1* (MIM 609678). Excessive hair pulling with crusting, pimples, tenderness, elevated scalp (Mirmirani and Khumalo, 2014) because of hairstyling practices causes traction alopecia (Xu *et al.*, 2017) In discoid lupus erythematosus head and neck bear erythematous lesions and scales that leave scars and lead to hair loss that can't be

reversed (Arkin *et al.*, 2015; Xu *et al.*, 2017). Neonates develop patches on the occipital region and ensue transient neonatal hair loss and afterwards the hair re-grows (Cutrone and Grimalt, 2005; Kim *et al.*, 2011; Castelo-Soccio, 2014). In androgenetic alopecia hair is lost from the androgen-dependent scalp region i.e midfrontal, temporal, parietal, and vertex. Female pattern hair loss is a type of AGA that particularly affects females involving scalp thinning. The androgen receptor gene (*AR*; MIM 313700) mapped between chromosome Xq13 and Xp11 is reported to cause AGA (Gonzalez *et al.*, 2010; Migeon *et al.*, 2010; Kibar *et al.*, 2014).

Syndromic Forms of Alopecia

Hypotrichosis with Cone-Rod Dystrophy (HJMD)

A syndromic form of alopecia with the AR mode of inheritance is hypotrichosis with juvenile macular dystrophy (MIM 601553) also known as hypotrichosis with cone-rod dystrophy. It is distinguished by slight to complete scalp hair loss, together with retinal degeneration causing visual impairment (Sprecher *et al.*, 2001). Sequence variants are reported in 16 exons containing *CDH3* gene (MIM 114021) that encodes P-cadherins and is mapped to chromosome 16q21-q23.1. High expression in hair and retina is observed (Sprecher *et al.*, 2001; Ahmad *et al.*, 2016). *CDH3* gene mutations are also associated with a AR recessive disorder i.e. EEM syndrome (MIM 225280) (Kjaer *et al.*, 2005). EEM syndrome phenotypes unravels the role of P.cadherins in limb development, formation of hair and retina (Shimomura and Christiano, 2010).

Alopecia and Mental Retardation Syndrome

APMR (MIM 203650) is characterized as alopecia totalis. Patients affected with APMR have mental retardation and other symptoms. Eyelashes, eyebrows, pubic and axillary hair are lost. Three risk loci for AMPR1, 2 and 3 syndrome are localized on chromosome 3q26.q26, 3q26.3-q27.3 and 18q11.2-q12.2, respectively (John *et al.*, 2006; Wali *et al.*, 2006; Wali *et al.*, 2007).

Woodhouse Sakati Syndrome

Woodhouse Sakati Syndrome (WSS; MIM 241080), a multisystem disorder is defined by hypotrichosis, hearing loss, extrapyramidal manifestations, diabetes, difficulty in

learning, and hypogonadism (Alazami *et al.*, 2008). It has been identified that the cause of WSS are the variations in the sequence of *DCAF17* (MIM 612515). Organ involvement in WSS is correlated with a *DCAF17* encoded nuclear protein with high expression in liver, skin and brain. Till date 12 sequence variants in *DCAF17* cause WSS (HGMD, 2021).

Ectodermal Dysplasias (ED)

Ectodermal dysplasias (ED) refers to the group of heritable diseases which are heterogenous in nature and characterized by genetic imperfections present in more than one ectodermal structure and their appendages i.e. hair, nails, teeth, sweat glands (Itin, 2014). There are two main groups of ectodermal dysplasias. In group one, due to failure of signaling between ectoderm and mesoderm, hypoplasia of ectodermal tissues is seen. Group 2, besides the other epithelial structures, palmoplantar keratoderma is the most significant feature. To date almost 200 different types of ED have been identified (Garcia-Martin *et al.*, 2013). In 75 different ectodermal dysplasias, a total of 77 genes and 9 chromosomal loci have been identified (Pagnan and Visinoni, 2014).

Palmoplantar Keratoderma

Hereditary palmoplantar keratodermas (PPKs) display hyperkeratosis of the soles and palms and belong to the group 2 of keratinization disorders (Priolo, 2009) that is phenotypically diverse and genetically heterogeneous. PPKs are inherited in all Mendelian inheritance patterns (AR, AD, X-linked, or mitochondrial) (Has and Technau-Hafsi, 2016). On the basis of the tissue involved, PPKs may be isolated or syndromic.

Thickening of only the palmoplantar skin is involved in isolated PPK whereas in the syndromic forms, along with the palmoplantar skin thickness, several other ectodermal structures/ extra-cutaneous tissue defects are also highlighted (Schiller *et al.*,2014). To date, 25 genes have been identified that are associated with the PPKs (Schiller *et al.*, 2014). Traditionally they are classified as;

- Hereditary palmoplantar hyperkeratosis
- Acquired palmoplantar hyperkeratosis

The major defects leading to hereditary PPKs are the ones that particularly disrupt intermediate filaments formed by keratin, gap junctions, desmosomes, water channels and EGFR signaling (Has and Technau-Hafsi, 2016). Drugs, chemicals, systemic disease, infections, dermatoses, malignancy and keratoderma climactericum are responsible for the acquired PPKs (Patel *et al.*,2007). On the basis of morphology and extent of hyperkeratosis on soles and palms, hereditary PPK have 4 major types; Diffuse, Focal, Striate, and Punctate PPK (Sakiyama and Kubo, 2016).

Diffuse Palmoplantar Keratoderma (DPPK)

DPPK is either AR or AD in which the entire surface of soles as well as palms is covered by diffuse hyperkeratosis. DPPK is divided into two types; DPPK with transgrediens and DPPK without transgrediens.

Diffuse PPK without Transgrediens

Unna– Thost PPK (MIM 600962) is the most common, non-epidermolytic AD form of diffuse PPK without transgrediens. It is instigated by mutation in *KRT9* (MIM 607606) *or KRT1* (MIM 139350) (Reis *et al.*,1994; Kuster *et al.*, 2002; Knöbel *et al.*, 2015). Nine exons containing *KRT1* localizes to chromosome 12q11-q13 (Popescu *et al.*, 1989) while 8 exons containing *KRT9* localizes to chromosome 17q21.1-q21.2 (Reis *et al.*,1994). To date 29 mutations in the *KRT9* and 42 in the *KRT1* are associated with PPK (HGMD, 2021).

Diffuse PPK with Transgrediens

Several diseases are associated with diffuse PPK with transgradiens. Mal de Meleda (MDM; MIM 248300), characterized by PPK, skin lesions, brachydactyly, and nail deformities, and mutation in *SLURP1* gene (MIM 606119) underlie MDM (Fischer, 2001). Nagashima type of PPK (PPKN; MIM 615598),), a non-progressive disorder without constricting bands and a variation is observed in PP hyperkeratotic skin on exposure to water (Nagashima, 1977). Mutation in *SERPINB7* (MIM 603357) lead to PPKN (Kubo *et al.*, 2013). Bothnian PPK (MIM 600231) an autosomal dominant form exhibiting spongy appearance upon water exposure. It shows a diffuse non-epidermolytic PPK (Lind *et al.*, 1994; Kubo *et al.*, 2013) and *AQP5* gene mutations (MIM 600442), that encodes a water channel protein, is responsible for PPKB (Blaydon

et al., 2013). Gamborg-Nielson PPK (PPK-GN; MIM 244850) caused due to *SLURP1* gene mutations (MIM 606119) (Zhao *et al.*, 2014) and displays hyperkeratosis at the knuckle pads without nail abnormalities (Kastl *et al.*, 1990). Greither PPK (MIM 144200) and Sybert PPK are the AD forms of DPPK. *KRT1* (MIM 139350) mutations underlie Greither PPK while gene for Sybert PPK is yet unknown (Gach*et al.*, 2005). Sybert PPK shows hyperkeratosis and in comparison to Greither is more severe (Sybert *et al.*, 1988). To date 17, 11 and 6 mutations are found in *SLURP1*, *SERPINB7* and *AQP5* gene, respectively underlying PPK.

Focal Palmoplantar Keratoderma

A pachyonychia congenita in which the individual's body weight-bearing area of the soles have hyperkeratosis like calluses (Kubo *et al.*, 2013). Mutations in *KRT6A* (OMIM 148041), *KRT6B* (OMIM 148042), *KRT16 (O*MIM 148067*)*, or *KRT17* (OMIM 148069), *KRT6C* (OMIM 612315), *DSG1* (OMIM 125670) and *TRPV3* (OMIM 607066) genes cause FPK (Eliason *et al.*, 2012; Wilson *et al.*, 2010). *TRPV3* gene mutations are also associated with Olmsted syndrome (MIM 614594), which also exhibit diffuse PPK and perioral hyperkeratosis, indicating *TRPV3* involvement in differentiation of keratinocytes (He *et al.*, 2015). To date, 16 mutations underlying PPK are reported in *TRPV3* gene (HGMD, 2021).

Striate Palmoplantar Hyperkeratosis

Thickening of skin on the soles and fingers particularly the pressure points is seen in the AD form of striate PPK. It is bifurcated into three types; PPKS I, PPKS II, PPKS III (Whittock *et al.*, 2002). Striate PPKSI is characterized by focal, diffused and striate PPK. Underlying cause is the mutation in a desmosomal component 15 exon containing *DSG1* gene (MIM 125670) that also leads to SAM syndrome (MIM 615508). So far 28 mutations are reported in DSG1 underlying PPKS. Striate PPKSII displays linear and focally distributed lesions on the palms because of the haploinsufficiency of desmoplakins (Has and Technau-Hafsi, 2016). The mutation in desmosomal plaque formation 24 exon containing *DSP* gene (MIM 125647) causes PPKSII. 3 mutations are reported in *DSP* gene underlying PPKS (HGMD, 2021). Striate PPKSIII is caused due to impaired hemidesmosomes and keratin filaments in suprabasal keratinocytes

(Whittock *et al.*, 1999). To date one mutation in *KRT1* gene (MIM 139350) lead to the PPKSIII phenotypes (HGMD, 2021).

Punctate Palmoplantar Keratoderma

On the basis of clinical and genetic basis, there are three types of puntate PPK that have autosomal dominant inheritance pattern: PPKPI (MIM 148600, 614936), PPKPII (MIM 175860) and PPKPIII (MIM 101850) (Brown, 1971; Has *et al.*, 2016). PPKP I or Buschke–Fischer–Brauer type is the phenotype displaying numerous tiny punctate keratosis on the soles and palms (Brauer, 1913). Lesion number as well as size is observed to increase progressively. *AAGAB* gene (MIM 614888) that encodes p34 protein (an alpha and gamma-adaptin binding protein) (Giehl *et al.*, 2012) and *COL14A1* (OMIM 120324) (Guo *et al.*, 2012) are the major causes of PPKP I. According to HGMD, 41 mutations in *AAGAB* and a single mutation in *COL14A1* are found underlying PPKP. Porokeratotic PPK or PPKPII shows keratotic spines of columnar parakeratosis on the palmoplantar surface. The genetic basis of PPKII are yet unknown (Brown, 1971). In PPKP III or acrokeratoelastoidosis the margins of feet and hands are covered by tiny keratotic papules. The disease causing gene is mapped on chromosome 2. Filaggrin (FLG; MIM 135490) overexpression is also reported to cause PPKPIII (Braun-Falco, 2009). The underlying genes for PPKPIII are yet to be identified (Has *et al.*, 2016).

The present study aimed to clinically and genetically characterize three Pakistani consanguineous families affected with syndromic and isolated forms of hair disorders and ectodermal dysplasia. One family with palmoplantar keratoderma and two with hair loss disorders were included. The study objectives includes assessing the disease phenotypes, inheritance pattern, identification of genes and the causative variants for pathogenesis of the disorders. Linkage analysis was carried via highly polymorphic microsatellite markers. In family A, linkage was tested to genes, including *HR, DSG4/DSC3, LPAR6* and *LIPH*. In family B, linkage was tested to genes, including *HR, DSG4/DSC3, LPAR6, LIPH* and *CDH3*. Both families failed to show linkage to the genes tested. In family C, linkage analysis was performed using polymorphic microsatellite markers associated with syndromic palmoplantar keratoderma genes, including *SERPINB7, JUP, DCAF17, NLRP1, GJB6, SDR9C7,* and *SLURP1*. However,

the family didn't manifest convincing linkage. Sanger sequencing of two previously candidate genes, *GJB6* and *GJA1*, in affected members in family B and C respectively, failed to identify the disease-causing variants. Exclusion of linkage to the known candidate genes in all three families depict involvement of the unknown novel genes in causing the diseased phenotypes. Use of whole-exome sequencing (WES) and SNP-microarray can facilitate in identifying the causative genes and the variants.

Chapter 2
Materials and Methods

MATERIALS AND METHODS

Study Subjects

The current study involved three families of Pakistani origin (A, B, C) that were presented with hereditary hair loss and ectodermal dysplasia. Family A and B belong to Noshera, Khyber Pukhtunkhwa, while family C belongs to a rural area located in Khuzdar, Baluchistan. To proceed the research, approval was granted by IRB (Institutional Review Board) of Quaid-i-Azam University, Islamabad. For blood collection, families were located and visited to their hometowns. Photographs of affected and normal individuals were also captured with their consent.

Pedigrees/Family Charts

Upon visit, the families were inquired about the thorough family history and clinical information. Further pedigrees were constructed to show that the families understudy segregate the disease in accordance with the Mendelian inheritance pattern. The questions regarding the disease onset and progression, severity, relationship between the couples suffering from the disease, and parents of the couple were asked from elders of the families. Pedigree construction was performed by the protocols set by Bernett *et al.* (1995). Pedigree design illustrates that the double lines indicated the consanguineous marriages, square denoted males while circles females, colorless circles and squares indicated normal members whereas the shaded ones symbolized the affected individuals. Square and circles crossed by inclined line represented the deceased members of the family. Roman numerals represented each subsequent generation when numbered from top to bottom. Within each generation the members and their relative positions were indicated by Arabic numerals.

Collecting Blood Specimens

Phlebotomy was performed on both the normal and affected individuals of the families. With the help of sterilized syringes particularly 10 ml (BD 0.8mm x 38mm 21G x 1 ½ TW, Franklin Lakes, USA), venous blood was drawn and to prevent the clotting, blood was immediately transferred to the EDTA (ethylene di-amine tetraacetate) containing vacutainer tubes (BD vacutainer K3-EDTA, Franklin Lakes, USA). Before DNA

extraction was proceeded, the collected blood samples were stored at 4°C in Human Molecular Genetics Laboratory (HMGL) located in the Biochemistry Department, Quaid-i-Azam University, Islamabad, Pakistan.

Genomic DNA Extraction

Extraction of the DNA was performed by the help of manual phenol chloroform method and also using the commercially available kit.

DNA Extraction by Phenol-Chloroform Method

Blood stored at 4°C was first subjected to one hour incubation before extracting DNA. From the whole blood, genomic DNA was extracted by following the standard protocol for the phenol chloroform method (Sambrook *et al.*, 1989).

i. The first step was to settle down the blood components at the bottom. For this purpose, the vacutainers containing blood samples were given an incubation time of about 20-30 minutes at room temperature.

ii. After the incubation, an equal volume of blood and solution A (750 µl each) were mixed together in an eppendorf tube of 1.5 ml (Oxygen, Union, USA). A thorough mixing of both components was done at room temperature by giving it an incubation time of 20-30 minutes.

iii. Centrifugation was done for 1 minute on 13,000 rpm (rotation per minute).

iv. After centrifugation, a pellet was seen particularly at the tube bottom. The supernatant was discarded from tube and re-suspension of the pellet was done by adding 400 µl of solution A to clear out the remaining blood cells from the pellet.

v. Another round of centrifugation was given for a time of at 13,000 rpm for about 1 minute.

vi. After disposing of the supernatant, pellet was obtained that was dissolved in solution B (400 µl), 20% SDS (Sodium Dodecyl Sulphate, 16 µl) and proteinase K enzyme (PK, 16 µl).

vi. Incubation of the mixture at 37°C for overnight was carried to completely dissolve the pellet.

vii. On the second day, a mixture of fresh solution C, along with solution D in equal amounts (250 µl each) was added in the tubes containing the dissolved pellets.

ix. At 13,000 rpm, the tubes were then centrifuged for a time of 10 minutes. Upon centrifugation, three distinguishable layers were obtained.

x. In a separate labeled tube, the upper layer was collected and 500 µl of solution D was added and mixed with it.

xi. For 1 minute, centrifuge the mixture at 13,000 rpm. Two separate layers were obtained. Precipitation of DNA in the form of threads was carried out after collecting the upper layer in a separate labeled tube and then added sodium acetate (55 µl) and isopropanol (500 µl).

xii. Centrifugation of the mixture at 13,000 rpm was caried out for 10 minutes. Followed by centrifugation, at the bottom of the tube, DNA pellet was vividly observed.

xiv. After removing residual mixture from the tube, washing of DNA pellet was performed with 250 µl of 70% ethanol (BDH, Poole, England) through centrifugation at 13,000 rpm for 7 minutes.

xv. After the centrifugation, the residual ethanol was removed. Using the vacuum concentrator 5301 (Eppendorf, Hamburg, Germany) the pellet was dried for 20 minutes at 45°C.

xvi. About 150-18 0µl of TE buffer solution (Sigma-Aldrich, St Louis, MO, USA) was added to the tube containing dried pellet and then incubated at 39°C for overnight to dissolve the pellet in the buffer.

xvii. 1% Agarose gel was used for visualization and analysis of the extracted DNA using the UV Transilluminator (Biometra, Gottingen, Germany). For the future use, the extracted DNA stock was stored at 4°C.

Table 2.1 Composition of Solutions Used in Genomic DNA Extraction

Solutions	Composition
Solution A	10mM Tris HCl (pH=7.5), 1% v/v TritonX-100, 5 mM $MgCl_2$, 0.32 M Sucrose
Solution B	10mM Tris HCl (pH=7.5), 400mM NaCl, 2mM EDTA (pH=8.8), Distilled water
Solution C	Saturated Phenol
Solution D	Isoamylalcohol: Chloroform (1:24)
Sodium Acetate	3M Sodium Acetate (trihydrate, pH 6), autoclaved distilled water
20% SDS	10g Sodium Dodecyl Sulphate in 40 ml distilled water
70% Ethanol	Absolute Ethanol (70ml), in 30ml of distilled water
DNA dissolving buffer	10 mM Tris (pH=7.5), 0.1 mM EDTA (pH=8.0)
Bromophenol Blue	40 g Sucrose, 0.25 g Bromophenol Blue

DNA Extraction Using Commercially Available Kit Procedure

Commercially available Kit Sigma- Aldrich (Gene-Elute Blood Genomic DNA kit) was also used for the extraction of genomic DNA.

i. In a tube of 1.5 ml, blood (200 µl), lysis buffer (200 µl) and PK enzyme (20 µl) were added together and thoroughly mixed.

ii. An incubation time of 10 minutes for 55°C was given to the mixture in a water bath.

iii. 200 µl of 100% chilled ethanol was put into the mixture and then vortexed for 15 seconds. At 3,000 rpm, a short spin was given to the mixture and then transferred to the column (Sigma-Aldrich USA).

iv. Centrifugation was performed at 8,000 rpm for 1 minute and then the columns were transferred to other tubes.

v. After that, washing was done twice by upon addition of 500 µl of AW washing buffer and then centrifuged at 13,000 rpm each time.

To dry the columns, an empty spin was given and then elution buffer (240 µl) was added to the columns. This was followed 10 minutes incubation at room temperature.

vi. DNA was then eluted from the columns into tubes by centrifugation at full speed.

Agarose Gel Electrophoresis (1%)

The extracted DNA from the blood samples was analyzed both quantitatively and qualitatively with the help of agarose gel electrophoresis using 1% agarose gel. At first, 1 g of agarose was added in 10X TBE and distilled water (10 ml: 90 ml). Heating the agarose in the microwave oven for a time of 1-2 minutes dissolves the agarose. After the agarose was dissolved completely, 5 µl of ethidium bromide (staining dye) was mixed in agarose. To create the wells for DNA loading, combs were placed in the tank before pouring the solution. After thorough mixing of the dye in agarose solution, the solution was then poured into the gel tank carefully. In order to solidify, the gel was left at room temperature for 30 mints. DNA (4 µl) mixed with loading dye (4 µl) was loaded into the gel. TBE buffer (1X) was added to the gel tank in which gel was placed. For 40-50 minutes, electrophoresis was performed at 120 volts. Using the U.V Trans-illuminator (Biometra, Gottingen, Germany), DNA bands visualization was carried out. With a Digital Camera EDAS 290 (Kodak, New York, USA), the photographs were taken that analyzed the DNA presence along with the DNA quality.

Table 2.2 Composition of Solutions Used in Agarose Gel Preparation

Solutions	Compositions
Gel preparing buffer (10X TBE)	54.8 g Tris, 27.5 g Boric acid, 3.65 EDTA (pH=8.3), 500ml water
Gel running buffer (1X TBE)	10X TBE: Distilled water (1:9)
Ethidium Bromide (100 ml)	1g Ethidium bromide in 100 ml autoclaved distilled H_2O
Loading dye	40 g Sucrose + 0.25 g Bromophenol Blue
T.E buffer	1M Tris HCl (pH 7.5), 0.5M EDTA (pH 8), autoclaved distilled water
Distilled Water	90 ml

DNA Quantification

Quantity of DNA in the DNA samples was calculated using a Colibri micro-volume spectrophotometer (Titertek Berthold, Germany) in which an optical density (OD) of 260 nm wavelength was taken. The instrument was blanked by adding 1µl of TE buffer. After that, 1 µl of the DNA sample was loaded in the instrument to measure its concentration in ng/µl units.

Genotyping and Linkage Analysis/Homozygosity Mapping

The families with hereditary hair disorder and ectodermal dysplasia were subjected to linkage analysis using microsatellite markers specific for the genes known to cause the associated phenotypes. Information regarding the genes tested in the research was obtained from the human GRChg/hg19 assembly of the UCSC genome browser. Table 2.5 lists the microsatellite markers used for genotyping. Markers used in present study were selected having an average heterozygosity >80%. Marker's genetic distances were obtained from Rutgers's combined linkage physical map of the human genome (Matise *et al.*, 2007). PCR (Polymerase Chain Reaction) is the final procedure employed for the microsatellite markers analysis.

PCR Amplification

Polymorphic microsatellite markers were used for the amplification purpose. Following the standard procedure, 25 µL volume was prepared that contained 1 µL of DNA and 23-24 µL of the reaction mixture in 200 µL PCR tubes (Axygen, California, USA). The concentration of the chemicals used in the PCR reaction are given in Table 2.3. PCR reaction was carried out via T3 Thermocycler (Biometra, Germany) and GENE Amp PCR system 9600 (Perkin Elmer, Wellesley, MA, USA). 8% polyacrylamide gels are used for the resolving the amplified products. Ethidium bromide stained the gel. Further, bands were visualized and analyzed by UV trans illuminator.

Table 2.3 Chemicals Used in PCR master mix

Chemicals Used	Amount Used in PCR
DNA Dilution	2.0 µL
PCR Buffer -10-X (200 Mm $(NH4)_2$ SO4 + 750 mM Tris-HCl) (MBI Fermentas, Life Sciences, UK)	2.5 µL
25 mM $MgCl_2$	2.0 µL
10 mM dNTPs	0.5 µL
20 ng/ µL Forward Marker	0.3-0.4 µL
20 ng/ µL Reverse Marker	0.3-0.4 µL
PCR Water	17.3 µL
0.5 U/ µL Taq Polymerase (Perkin-Elmercetus, Ferments, Burlington, Canada).	0.3 µL

Polyacrylamide Gel Electrophoresis (PAGE)

The products amplified by PCR were resolved using the 8% non-denaturing polyacrylamide gel. Preparation of single gel plate required addition of 50 ml solution in 500 ml graduated cylinder. Chemicals used for polyacrylamide gel preparation are listed in Table 2.4. Between the two glass plates, that were 1.5 mm distance apart, the solution that was prepared was then poured. After pouring, comb was inserted between the gel plates. Gel was polymerized and subsequent solidification occurred after about 40-60 minutes at room temperature. The DNA sample, before loading into the gel wells,

was mixed with loading dye (6 µl). By the use of a vertical gel tank (Whatman, Biometra, Gottingen, Germany) containing 1X TBE buffer, at about 120 volts, an electrophoresis reaction was carried out for 120-150 minutes. Ethidium bromide stained the gel and UV transilluminator (Biometra, Gottingen, Germany) was used for visualization purpose and for capturing the photograph Digital camera DC 290 (Kodak, Digital Sciences, New York, USA) was used.

Table 2.4 Composition and Concentration of Chemicals Used in Polyacrylamide Gel

Chemicals Used	Composition	Amount Used in PCR
30% Acrylamide	Acrylamide (MERCK Darmstadt, Germany), N,N Methylene -bisacrylamide (29:1)	13.5 mL
10X TBE	Tris 0.89 M + Borate 0.89 M + EDTA 0.02 M	5 mL
10% APS	Ammonium Sulphate (5 g/45mL distilled water)	400 µL
TEMED	N, N, N', N'-Tetra methyl ethylene diamine (Sigma-Aldrich, USA).	25 µL
Distilled Water		Raised to 50 µL

Sanger Sequencing of Genomic DNA

Based on previous reports of association of *GJB6* and *GJA1* with hair loss and palmoplantar respectively, the same genes were sequenced in DNA of affected and normal members using gene specific primers. For exons amplification two types of PCRs were performed.

First Sequencing PCR or Pre-sequencing PCR including

For the amplification of *GJB6* and *GJA1*, the reaction mixture was carried out in 200µl of PCR tube and reaction mixture of total 50 µl was prepared. PCR buffer (5 µl) together with template DNA (2.5 µl) plus forward and reverse primer (2.5 µl each) and $MgCl_2$ (3 µl) including dNTPs (1 µl) as well as Taq polymerase (0.7 µl) and PCR water (31.8 µl).

PCR tube was congregated in thermos cycler and the reaction was carried out by using same conditions as previously performed. 2% agarose gel present in 1X TBE (running buffer) was used for the verification of the product (exon amplification). PCR product (3 µl) together with bromophenol blue (3 µl) was loaded into the gel wells and run horizontally for 35 minutes at 110 volts.

First Purification of Amplified PCR products

When the amplification was confirmed on 2% agarose gel by visualizing gel bands the PCR products was purified by using Axygen Biosciences PCR Cleanup Kit (Invitrogen). Following steps were carried out during purification.

- To the tube containing the amplified PCR product, 120 µl of binding buffer solution (buffer A) was added and then vortex thoroughly. Mixture was poured in column, assembled in 2 ml collection tube and centrifugation was carried out at 13000 rpm/1 minute. Afterwards the liquid that flowed through the column was discarded.
- Washing of the column was performed with 500 ul ethanol-added washing buffer twice followed by centrifugation for about 1 mint at 13000 rpm.
- After discarding waste that was present in the collection tube, column was placed again in the tube and subsequent centrifugation carried out at 13,000 rpm for 2 mints for eliminating residuals.
- Column was then further transferred to a freshly labeled collection tube and elution buffer (25 µl) kept at 70°C was added.
- After 7 mints incubation, the centrifugation was performed (13,000rpm/3 min) and the purified product was finally collected in an eppendorf tube.

The product purified by the above procedure was evaluated by running on 2% agarose gel. DNA (3 µl) and loading dye (3µl) were loaded together onto the gel.

Primer Designing

Primers were designed for coding exons of *GJB6* and *GJA1* using online available "Primer 3" software (http://frodo.mit.edu/primer3/). For checking the effect of variant in *GJB6* and *GJA1*, primers were designed from exonic regions of *GJB6* and *GJA1*

using Integrated DNA Technologies (https://eu.idtdna.com/pages). Properties of amplified products were checked by UCSC and Ensemble genome browsers. The primer sequences are listed in table 2.6 and 2.7.

Analysis of Sequencing Data and Variant Validation

The sequencing data obtained after Sanger Sequencing was analyzed by software BioEdit alignment editor version 7.1.3.0 (http://mbio.ncsu.edu/BioEdit/bioedit.html). For the nucleotide linkage determination, chromatogram of afflicted was evaluated with the normal gene sequence (taken as a reference) which was retrieved from Ensemble Genome Browser Database (http://www.ensembl.org/index.html). Additionally, if variation was documented in the sequence of affected members, its pathogenicity was checked through MutationTaster (http://www.mutationtaster.org) or Polyphen-2 software (http://genetics.bwh.harvard.edu.pph2).

Table 2.5 List of microsatellite markers used for linkage analysis of candidate gene/loci

Sr. No.	Gene/ Loci	Chromosomal Position	Markers Used	cM
1.	***DCAF17***	2q31.1	D2S376	178.77
			D2S2284	179.17
			D2S2302	179.75
			D2S1267	181.62
			D2S1274	182.91
2.	***LIPH***	3q27.2	D3S1521	190.2
			D3S1571	192.93
			D3S3573	193.97
			D3S3592	195.04
			D3S1530	196.01
3.	***HR***	8p21.3	D8S1116	41.9
			D8S1861	42.82
			D8S136	43.63
			D8S1752	45.12
			D8S1734	45.12
4.	***SLURP1***	8q24.3	D8S1520	169.79
			D8S373	171.32
			D8S2334	171.32
			D8S1926	172.62
			D8S1108	172.62
5.	***SDR9C7***	12q13.3	D12S1632	72.58
			D12S90	73.71
			D12S305	73.31
			D12S1298	74.31
			D12S1056	75.09
6.	***GJB6***	13q12.11	D13S1316	0
			D13S175	0.55
			D13S633	3.1
			D13S1275	6.97
			D13S787	8.75

7.	***LPAR6***	13q14.2	D13S161	51.37
			D13S1269	53.19
			D13S268	54.17
			D13S788	54.17
			D13S1325	54.26
8.	***CDH3***	16q22.1	D16S3141	87.07
			D16S3067	87.07
			D16S3095	87.61
			D16S752	88.19
			D16S681	88.19
9.	***NLRP1***	17p13.2	D17S1828	10.34
			D17S1876	11.48
			D17S1854	13.1
			D17S1832	15.39
			D17S678	15.65
10.	***JUP***	17q21.2	D17S902	69.32
			D17S965	69.32
			D17S1860	69.99
			D17S579	69.99
			D17S934	69.99
11.	***DSG4/DSC3***	18q12.1	D18S49	53.51
			D18S36	54.83
			D18S47	54.83
			D18S456	55.74
			D18S536	56.29
12.	***SERPINB7***	18q21.33	D18S465	91.77
			D18S483	91.77
			D18S382	92.61
			D18S875	93.74
			D18S367	93.96

Table 2.6 List of primer sequences to PCR-amplify *GJB6*

Exon	Forward primer (F) (Nucleotide Sequence 5'-3')	Reverse primer (R) (Nucleotide Sequence 5'-3')
1	ACCTGGCCAAACATGAGAAT	GGGGTCAATCCCACATTTC

Table 2.7: List of primer sequences to PCR-amplify *GJA1*

Exon	Forward primer (F) (Nucleotide Sequence 5'-3')	Reverse primer (R) (Nucleotide Sequence 5'-3')
1	AGAAATACGTGAAACCGTTGGT	CACCGGATCAAAATTAACACCT

Chapter 3
Results

RESULTS

Recruitment of Families

Three families showing various types of skin disorders were recruited from different parts of the country for the study presented in the dissertation.

Family A

Family A, identified with alopecia, was sampled from Tehsil Pabbi located in Nowshera, Khyber Pakhtunkhwa province, Pakistan. Pedigree drawing shows that it is composed of three generations exhibiting autosomal recessive pattern of inheritance of the alopecia resulted from a consanguineous marriage (Figure 3.1). The first generation contains normal parents while the 2nd generation contains 2 carrier individuals, including a male and a female, and 11 other normal members. The 3rd generation has one affected male (III-3) and four normal individuals.

Affected member (III-3) in the family presented clinical features of a non-syndromic alopecia. He showed no other diseased phenotypes (Figure 3.2). Teeth, nails, and sweating were unaffected. For DNA analysis, blood was sampled from three individuals, including carrier parents (II-8, II-9) and an affected (III-3). These three members were represented with asterisk (*) in the pedigree drawing (Figure 3.1).

Family B

Similar to the family A, this family was also originated from Nowshera, Khyber Pakhtunkhwa. It was identified that the family segregated a syndromic form of congenital alopecia. A four generations pedigree (Figure 3.3) was constructed for this family. Upon pedigree analysis, it was revealed that the pedigree showed autosomal recessive inheritance pattern with consanguineous marriages. Generation III contains 2 male alopecia patients (III-7, III-9), 4 carrier individuals (III-10, III-11, III-13, III-14) and 8 normal individuals. In the 4th generation 2 alopecia patients (IV-7, IV-8) resulted from the carrier parents in the 3rd generation.

The affected members have sparse hair especially on the scalp as well as eyebrows, eyelashes, and beard hair. Wooly hair phenotype was also associated with the disease.

Whitish discoloration of the nails (onycholysis) with hypodontia wee exhibited by the patients. Blood was drawn from five members, including two carriers (III-10, III-11) and three affected (III-7, IV-7, IV-8). Molecular analysis of the extracted DNA was carried out as described below.

Family C

Family C is an inhabitant of a rural area located in Khuzdar, Baluchistan province of the country. Affected members in the family segregated palmoplantar keratoderma in autosomal recessive manner. The four generations pedigree was constructed after collecting required information from elders in the family (Figure 3.5). It consists of 22 members, including 8 affected (III-6, IV-1, IV-2, IV-3, IV-8, IV-9, IV-10, IV-11).

Clinical examination of the affected members presented palmoplantar keratosis with thick waxy skin. Careful examination revealed presence of hyperkeratotic plaques on the pressure points of soles, palms, ankles and between the digits in the affected members. In addition, they displayed chipped tooth and mild hammertoes. One of the affected members (III-6) exhibited an additional feature of pre-axial polydactyly. For DNA analysis, blood samples were provided by seven family members, including one normal (III-1), two carriers (III-3, III-4), and four affected (III-6, IV-1, IV-2, IV-3).

Mapping Candidate Genes Involved in Causing Alopecia and Ectodermal Dysplasia

To search for the causative genes and sequence variants in each of the three families, genomic DNA extracted from affected and unaffected members' blood was subjected to genotyping using polymorphic microsatellite markers linked to the previously known genes for alopecia and palmoplantar keratoderma. In all, 12 candidate genes were tested for linkage in the three families. These included, *DCAF17* (2q31.1), *LIPH* (3q27.2), *HR* (8p21.3), *SLURP1* (8q24.3), *SDR9C7* (12q13.3), *GJB6* (13q12.11), *LPAR6* (13q14.2), *CDH3* (16q22.1), *NLRP1* (17p13.2), *JUP* (17q21.2), *DSG4/DSC3* (18q12.1), and *SERPINB7* (18q21.33).

A list of microsatellite markers used to test linkage is provided in the table 2.5. As described in the previous chapter, PCR was performed using the standard protocol and

the products were then resolved on PAGE (8%) and stained with ethidium bromide. The confirmation of linkage of the family to the tested gene was based on the normal individuals exhibiting heterozygous and affected homozygous pattern of alleles.

In family A, DNA of three members including parents (II-8, II-9) and single affected (III-3) was genotyped using microsatellite markers tightly linked to previously reported alopecia causative genes. These included *HR* [D8S1116, D8S1861, D8S136, D8S1752, D8S1734], *DSG4/DSC3* [D18S49, D18S36, D18S47, D18S456, D18S536], *LPAR6* [D13S161, D13S1269. D13S268, D13S788, D13S1325], and *LIPH* [D3S1521, D3S1571, D3S3573, D3S3592, D3S1530]. Analysis of the genotyped markers failed to reveal homozygous pattern for alleles, indicating the family was not linked to any of the four candidate genes tested.

In family B, DNA of five members, including two normal (III-10, III-11) and three affected (III-7, IV-7, IV-8) was genotyped using microsatellite markers tightly linked to previously reported alopecia causative genes. This included *HR* [D8S1116, D8S1861, D8S136, D8S1752, D8S1734], *DSG4/DSC3 DSC3* [D18S49, D18S36, D18S47, D18S456, D18S536], *LPAR6* [D13S161, D13S1269. D13S268, D13S788, D13S1325], *LIPH* [D3S1521, D3S1571, D3S3573, D3S3592, D3S1530], and *CDH3* D16S3141, D16S3067, D16S3095, D16S752, D16S681. Based on the principle of linkage described above, the family failed to show linkage to the five genes tested.

Based on the clinical features, observed in affected members in the family C, linkage was tested with seven genes. This included *SERPINB7* [D18S465, D18S483, D18S382, D18S875, D18S367, *JUP* [D17S902, D17S965, D17S1860, D17S579, D17S934], *DCAF17* [D2S376, D2S2284, D2S2302, D2S1267, D2S1274], *NLRP1* [D17S1828, D17S1876, D17S1854, D17S1832, D17S678], *GJB6* [D13S1316, D13S175, D13S633, D13S1275, D13S787], *SDR9C7* [D12S1632, D12S90, D12S305, D12S1298, D12S1056], and *SLURP1* [D8S1520, D8S373, D8S2334, D8S1926, D8S1108]. DNA extracted from blood of six individuals, including two normal (III-1, -III-4) and four affected (III-6, IV-1, IV-2, IV-3) was subjected to genotyping. Similar to the results obtained in other two families, in the present case as well linkage was not found.

Sequencing Candidate Genes in Family B and C

In addition to testing microsatellite-based linkage to candidate genes, described above, two major causative genes were sequenced in an affected member in family B and C. Dideoxy chain termination method (Sanger Sequencing) was followed for sequencing the candidate genes. Protocol followed for sequencing the genes has been described in the chapter 2. Primers to PCR-amplify coding regions of the two genes were designed by Primer 3 software (http://frodo.mit.edu/primer3/) and listed in the Table 2.6 and Table 2.7.

In family B, *GJB6* gene containing single exon, located on chromosome 13q12.11, was sequenced in the affected member. In family C, however, another gene *GJA1* containing one exon, located on chromosome 6q22.31, was sequenced in the affected member. However, analysis of the sequencing data failed to reveal disease causing variants in both the families.

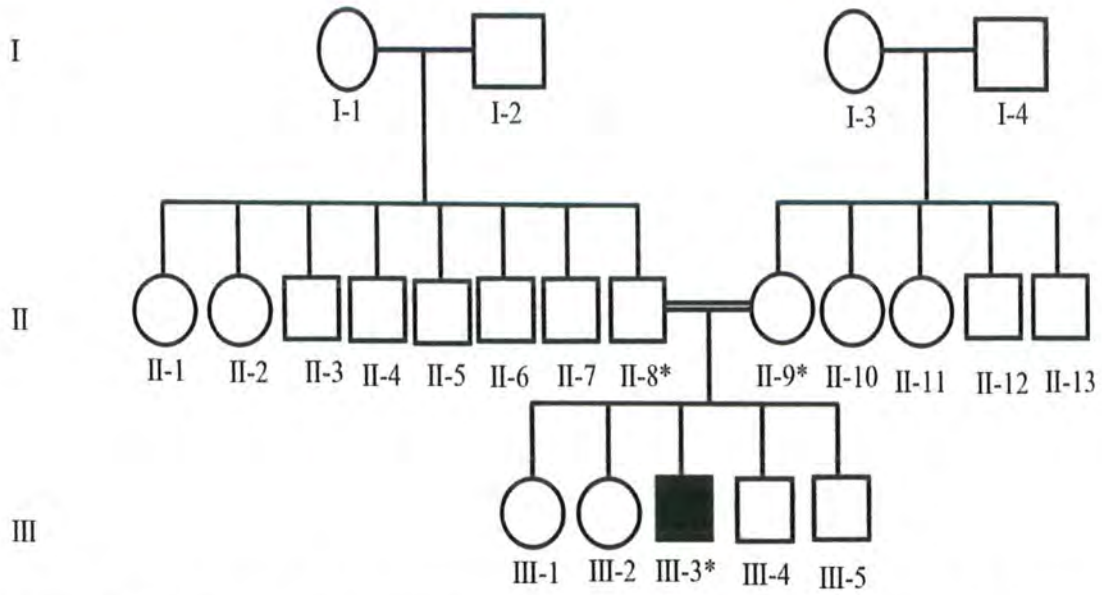

Figure 3.1: Pedigree of family A, segregating a non-syndromic form of alopecia. Circles indicate females and squares represent males. Affected members are denoted by shaded symbols whereas, unaffected members with the unshaded symbols Roman numerals reveal the generation number of individuals within a pedigree while Arabic numerals show the position of members within a generation. Asterisk (*) labeled shapes indicate the members whose blood is drawn.

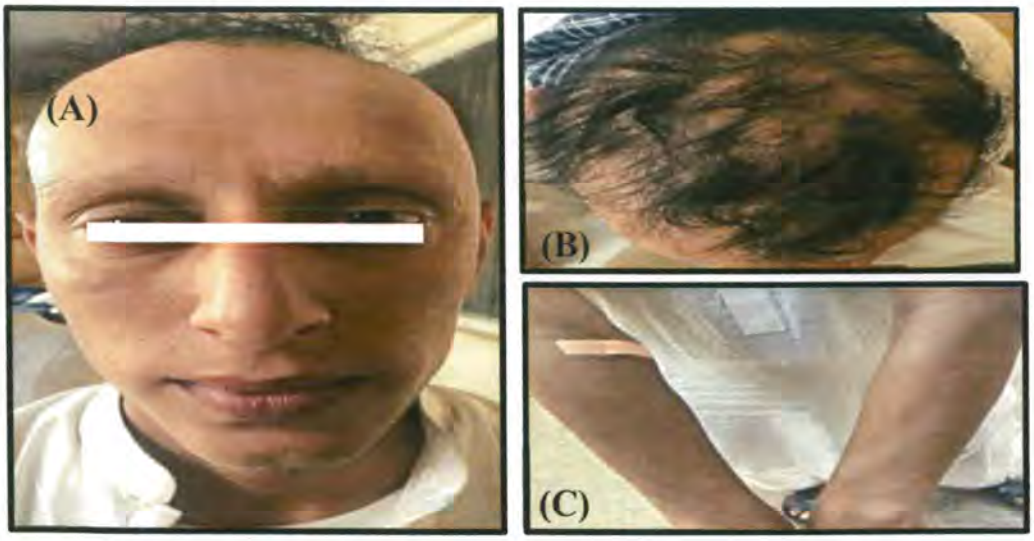

Figure 3.2: Affected individual (III-3) of family A displaying non-syndromic form of congenital alopecia. Images show sparse body hair (C) especially of the scalp (B), with absent eyebrows and eyelashes. Beard is also absent. Triangular shaped face is also seen in the above image (A). No other associated abnormalities were reported. Pictures were taken and presented here with the consent of the elders of family.

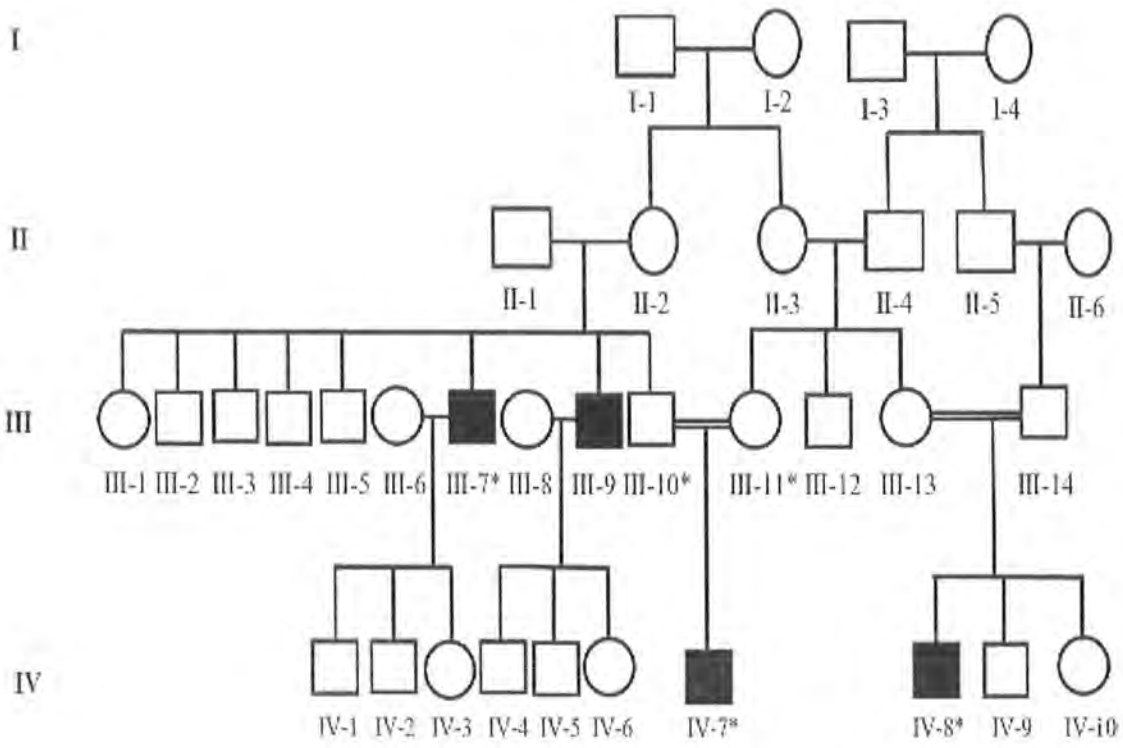

Figure 3.3: Pedigree chart of family B segregating a syndromic form of alopecia. Males are shown by squares while females by circles. Completely filled shapes illustrate the members with hypotrichosis while the unfilled ones represent the normal individuals. Double lines highlight the consanguineous unions. Roman and the Arabic numerals are used to represent the generation number and the members in the pedigree, respectively. Shapes with the asterisk (*) symbolize the members from whom the blood was collected.

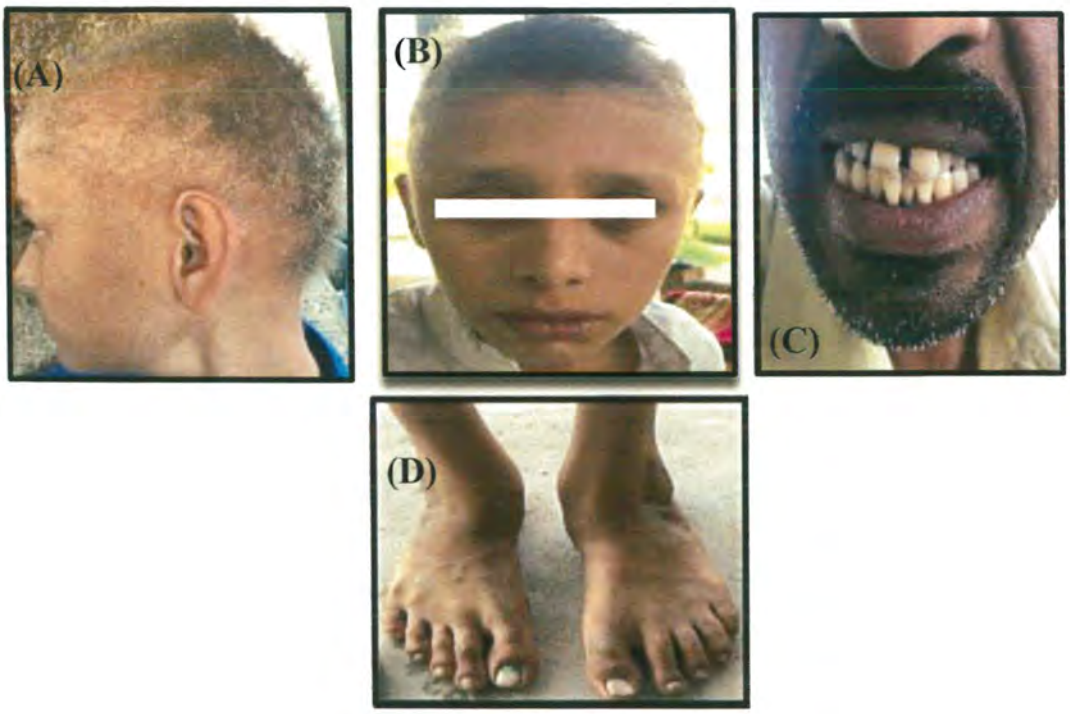

Figure 3.4: Affected individuals of the family B (III-7, III-9 IV-7, IV-9) displaying a syndromic form of alopecia. Images show that the patients have sparse wooly hair on the scalp (A). Eyelashes, eyebrows, and beard hair are also sparse (B, C). Hypodontia (C) and nail discoloration are also seen in the above pictures (D).

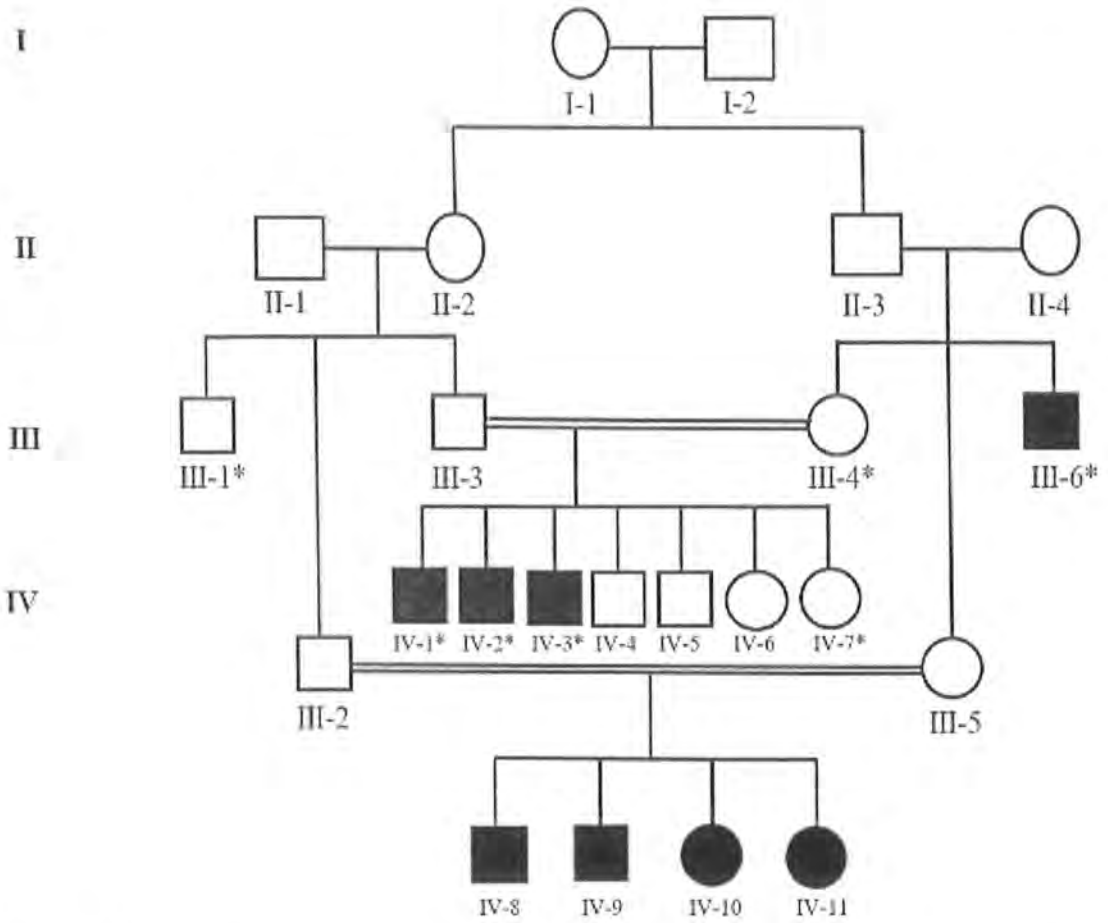

Figure 3.5: Pedigree sketch of family C with syndromic form of palmoplantar keratoderma having autosomal recessive pattern of Mendelian inheritance. Normal members are represented using the colorless symbols while affected members are symbolized by colored shapes. Double lines show the cousin marriages. The asterisk (*) marked individuals show the samples that are available for the study.

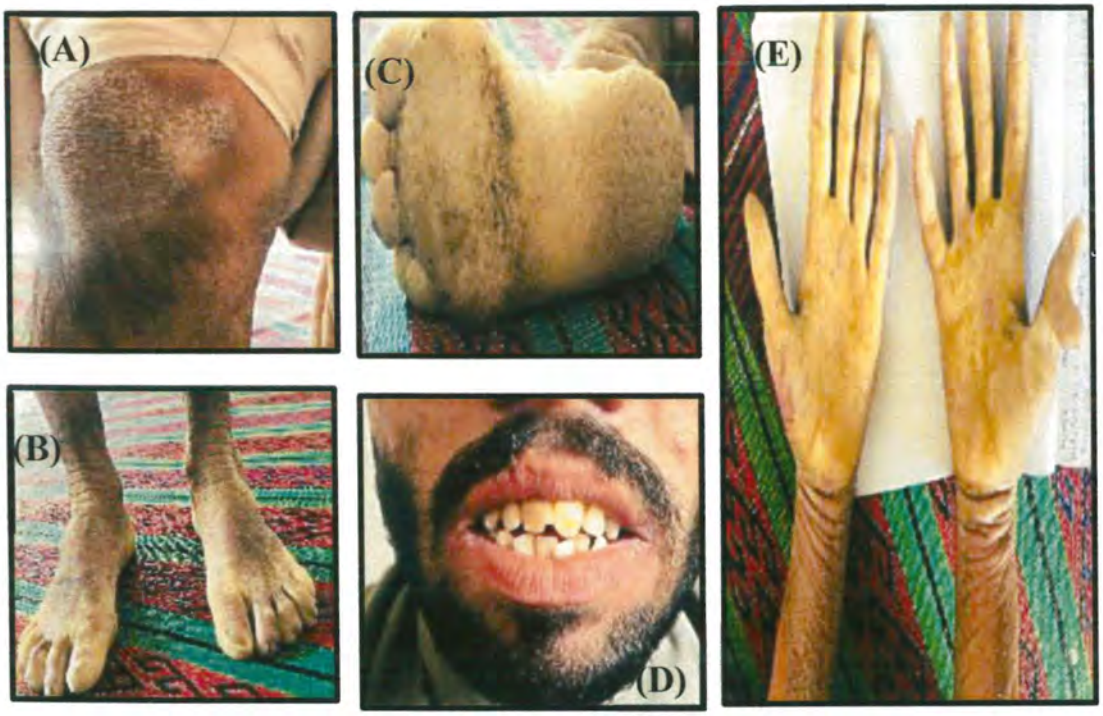

Figure 3.6: Affected individuals of the family B (III-6, IV-1, IV-2, IV-3) with clinical features of palmoplantar keratoderma (E). Diffuse PPK with trans-gradients showing hyperkeratotic plaques on ankles, knees, palms, and the soles surface are seen in the pictures (A, B, C). Hammertoes and chipped tooth phenotypes are also shown by the patients (D).

Sr. No.	Marker ID	Cytogenetic Position (cM)	1	2	3
1.	D3S1521	190.2			
2.	D3S1571	192.93	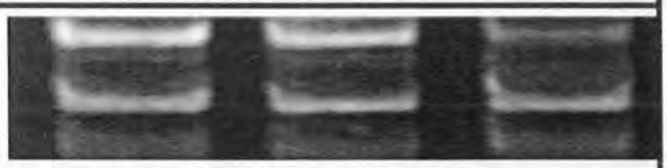		
3.	D3S3573	193.97	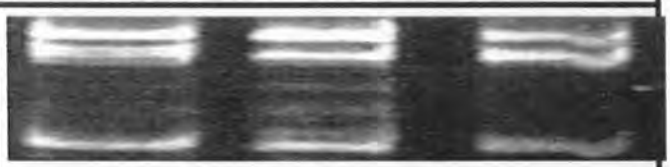		
4.	D3S3592	195.04	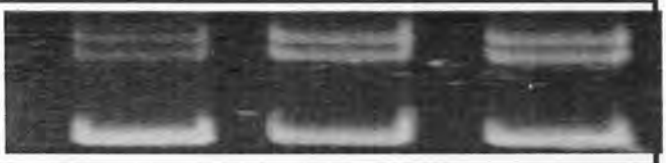		
5.	D3S1530	196.01	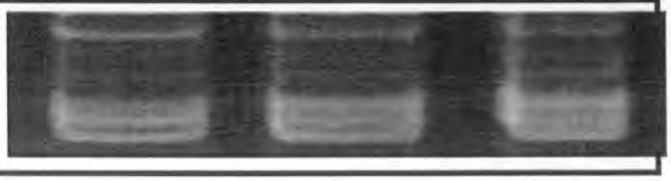		

Figure 3.7: The Electropherogram shows the allelic pattern of family A amplified using microsatellite markers flanking the *LIPH* gene on chromosome 3q27.2. Here, Lane 1 and 2 shows results for normal individuals (II-1and 2-II-2 while Lane 3 shows results for affected individuals (III-3). In the pedigree, Arabic numbers represent the postions of the individuals within a generation and Roman numerals specify the individual's number within the generation.

Sr. No.	Marker ID	Cytogenetic Position (cM)	1	2	3
1.	D8S1116	41.9	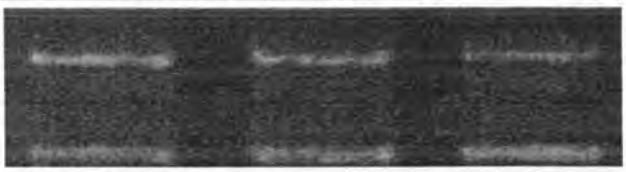		
2.	D8S1861	42.82	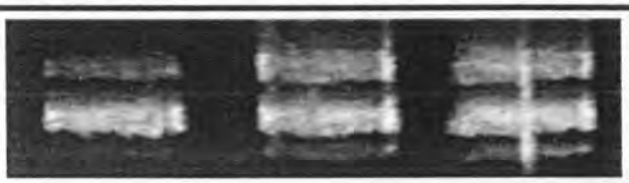		
3.	D8S136	43.63	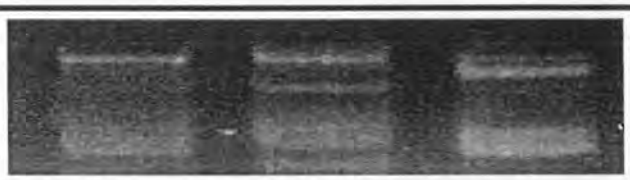		
4.	D8S1752	45.12	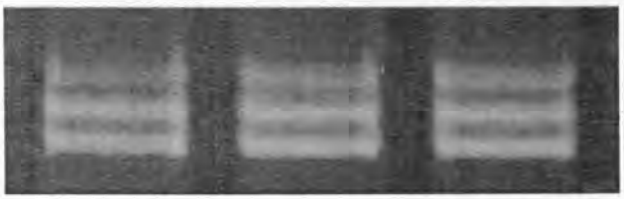		
5.	D8S1734	45.12			

Figure 3.8: The Electropherogram shows the allelic pattern of family A amplified using microsatellite markers flanking the *HR* gene on chromosome 8p21.3. Here, Lane 1 and 2 shows results for normal individuals (II-1and 2-II-2 while Lane 3 shows results for affected individuals (III-3). In the pedigree, Arabic numbers represent the postions of the individuals within a generation and Roman numerals specify the individual's number within the generation

Sr. No.	Marker ID	Cytogenetic Position (cM)	1	2	3
1.	D13S161	51.37			
2.	D13S1269	53.19			
3.	D13S268	54.17			
4.	D13S788	54.17			
5.	D13S1325	54.26	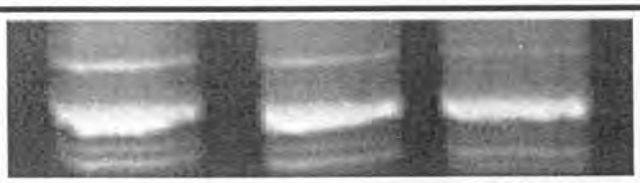		

Figure 3.9: The Electropherogram shows the allelic pattern of family A amplified using microsatellite markers flanking the *LPAR6* gene on chromosome 13q14.2. Here, Lane 1 and 2 shows results for normal individuals (II-1and 2-II-2 while Lane 3 shows results for affected individuals (III-3). In the pedigree, Arabic numbers represent the postions of the individuals within a generation and Roman numerals specify the individual's number within the generation.

Sr. No.	Marker ID	Cytogenetic Position (cM)	1	2	3
1.	D18S49	53.51			
2.	D18S36	54.83			
3.	D18S47	54.83			
4.	D18S456	55.74			
5.	D18S536	56.29	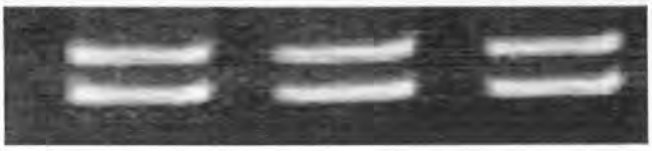		

Figure 3.10: The Electropherogram shows the allelic pattern of family A amplified using microsatellite markers flanking the *DSG4/DSC3* gene on chromosome 18q21.1. Here, Lane 1 and 2 shows results for normal individuals (II-1and 2-II-2 while Lane 3 shows results for affected individuals (III-3). In the pedigree, Arabic numbers represent the postions of the individuals within a generation and Roman numerals specify the individual's number within the generation.

Sr. No.	Marker ID	Cytogenetic Position (cM)	1	2	3	4	5
1.	D8S1116	41.9					
2.	D8S1861	42.82	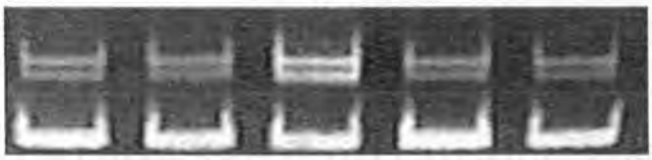				
3.	D8S136	43.63					
4.	D8S1752	45.12	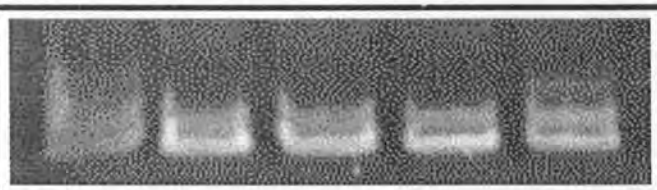				
5.	D8S1734	45.12	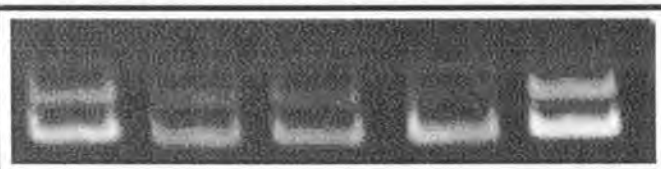				

Figure 3.11: The Electropherogram shows the allelic pattern of family B amplified using microsatellite markers flanking the *HR* gene on chromosome 8p21.3. Here, Lane 1 and 2 shows results for normal individuals (III-10 and III-11) while Lane 3, 4 and 5 shows results for affected individuals (III-7, IV-7, IV-8). In the pedigree, Arabic numbers represent the postions of the individuals within a generation and Roman numerals specify the individual's number within the generation.

Sr. No.	Marker ID	Cytogenetic Position (cM)	1	2	3	4	5
1.	D18S49	53.51					
2.	D18S36	54.83					
3.	D18S47	54.83					
4.	D18S456	55.74					
5.	D18S536	56.29	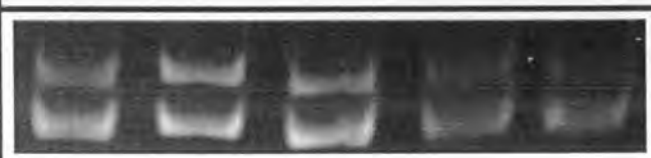				

Figure 3.12: The Electropherogram shows the allelic pattern of family B amplified using microsatellite markers flanking the *DSG4/DSC3* gene on chromosome 18q21.1. Here, Lane 1 and 2 shows results for normal individuals (III-10 and III-11) while Lane 3, 4 and 5 shows results for affected individuals (III-7, IV-7, IV-8). In the pedigree, Arabic numbers represent the postions of the individuals within a generation and Roman numerals specify the individual's number within the generation.

Sr. No.	Marker ID	Cytogenetic Position (cM)	1	2	3	4	5
1.	D13S161	51.37					
2.	D13S1269	53.19	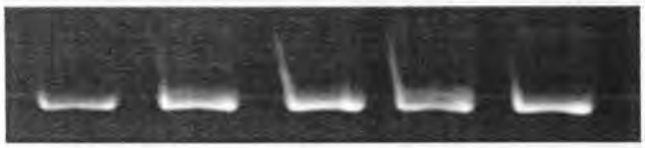				
3.	D13S268	54.17					
4.	D13S788	54.17	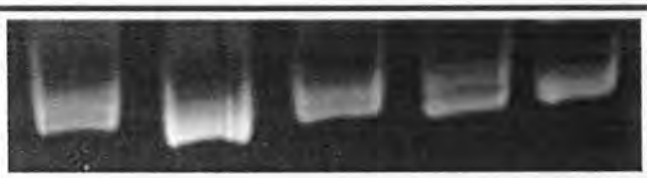				
5.	D13S1325	54.26					

Figure 3.13: The Electropherogram shows the allelic pattern of family B amplified using microsatellite markers flanking the *LPAR6* gene on chromosome 13q14.2. Here, Lane 1 and 2 shows results for normal individuals (III-10 and III-11) while Lane 3, 4 and 5 shows results for affected individuals (III-7, IV-7, IV-8). In the pedigree, Arabic numbers represent the postions of the individuals within a generation and Roman numerals specify the individual's number within the generation.

Sr. No.	Marker ID	Cytogenetic Position (cM)	1	2	3	4	5
1.	D3S1521	190.2					
2.	D3S1571	192.93					
3.	D3S3573	193.97					
4.	D3S3592	195.04					
5.	D3S1530	196.01	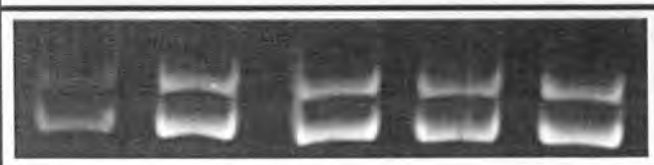				

Figure 3.14: The Electropherogram shows the allelic pattern of family B amplified using microsatellite markers flanking the *LIPH* gene on chromosome 3q27.2. Here, Lane 1 and 2 shows results for normal individuals (III-10 and III-11) while Lane 3, 4 and 5 shows results for affected individuals (III-7, IV-7, IV-8). In the pedigree, Arabic numbers represent the postions of the individuals within a generation and Roman numerals specify the individual's number within the generation.

Sr. No.	Marker ID	Cytogenetic Position (cM)	1	2	3	4	5
1.	D16S3141	87.07					
2.	D16S3067	87.07					
3.	D16S3095	87.61					
4.	D16S752	88.19					
5.	D16S681	88.19					

Figure 3.15: The Electropherogram shows the allelic pattern of family B amplified using microsatellite markers flanking the *CDH3* gene on chromosome 16q21.1. Here, Lane 1 and 2 shows results for normal individuals (III-10 and III-11) while Lane 3, 4 and 5 shows results for affected individuals (III-7, IV-7, IV-8). In the pedigree, Arabic numbers represent the postions of the individuals within a generation and Roman numerals specify the individual's number within the generation.

Sr. No.	Marker ID	Cytogenetic Position (cM)	1	2	3	4	5	6
1.	D2S376	178.77						
2.	D2S2284	179.17						
3.	D2S2302	179.75	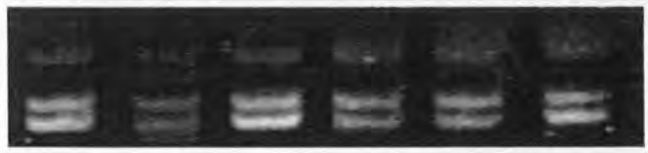					
4.	D2S1267	181.62	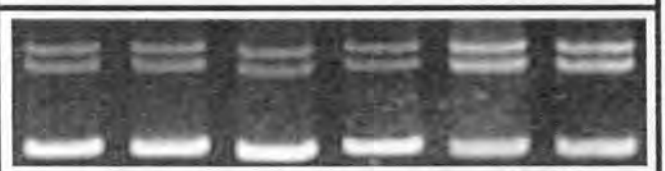					
5.	D2S1274	182.91	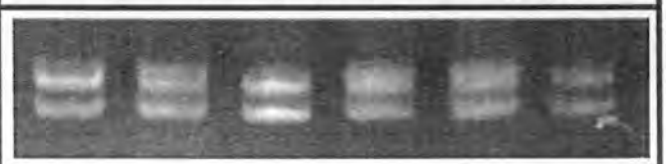					

Figure 3.16: The Electropherogram shows the allelic pattern of family C amplified using microsatellite markers flanking the *DCAF17* gene on chromosome 2q31.1. Here, Lane 1 and 2 shows results for normal individuals (III-1 and III-4) while Lane 3, 4, 5 and 6 shows results for affected individuals (III-6, IV-1, IV-2, and IV-3). In the pedigree, Arabic numbers represent the postions of the individuals within a generation and Roman numerals specify the individual's number within the generation.

Sr. No.	Marker ID	Cytogenetic Position (cM)	1	2	3	4	5	6
1.	D8S1520	169.79	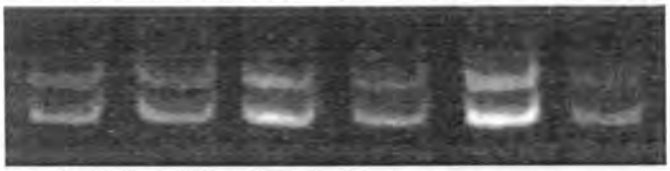					
2.	D8S373	171.32						
3.	D8S2334	171.32						
4.	D8S1926	172.62	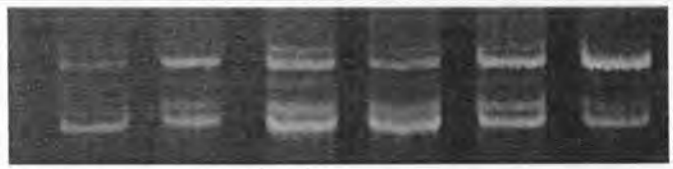					
5.	D8S1108	172.62	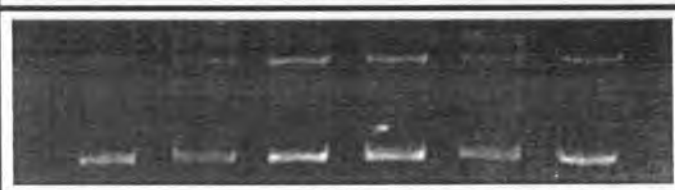					

Figure 3.17: The Electropherogram shows the allelic pattern of family C amplified using microsatellite markers flanking the *SLURP1* gene on chromosome 8q24.3. Here, Lane 1 and 2 shows results for normal individuals (III-1 and III-4) while Lane 3, 4, 5 and 6 shows results for affected individuals (III-6, IV-1, IV-2, and IV-3). In the pedigree, Arabic numbers represent the postions of the individuals within a generation and Roman numerals specify the individual's number within the generation.

Sr. No.	Marker ID	Cytogenetic Position (cM)	1	2	3	4	5	6
1.	D12S1632	72.58	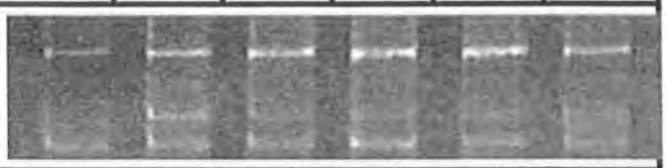					
2.	D12S90	73.71	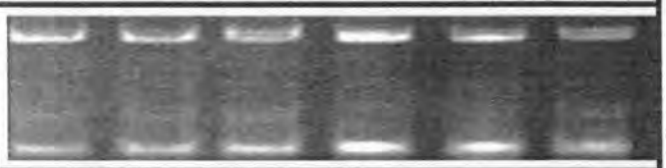					
3.	D12S305	74.31	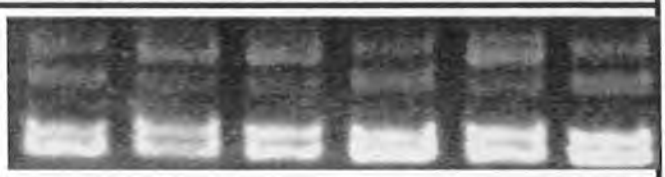					
4.	D12S1298	74.31	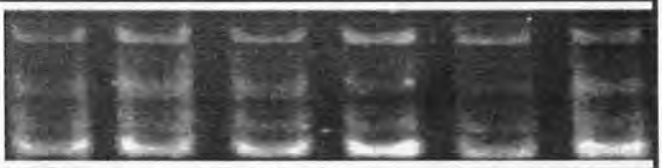					
5.	D12S1056	75.09	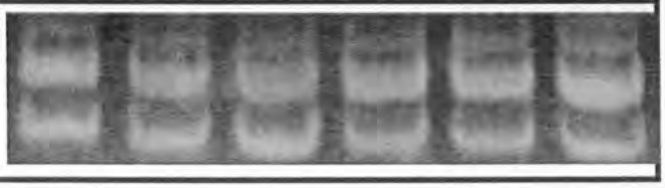					

Figure 3.18: The Electropherogram shows the allelic pattern of family C amplified using microsatellite markers flanking the *SDR9C7* gene on chromosome 12q13.3. Here, Lane 1 and 2 shows results for normal individuals (III-1 and III-4) while Lane 3, 4, 5 and 6 shows results for affected individuals (III-6, IV-1, IV-2, and IV-3). In the pedigree, Arabic numbers represent the postions of the individuals within a generation and Roman numerals specify the individual's number within the generation.

Sr. No.	Marker ID	Cytogenetic Position (cM)	1	2	3	4	5	6
1.	D13S1316	0						
2.	D13S175	0.55						
3.	D13S633	3.1						
4.	D13S1275	6.97						
5.	D13S787	8.75						

Figure 3.19: The Electropherogram shows the allelic pattern of family C amplified using microsatellite markers flanking the *GJB6* gene on chromosome 13q12.11. Here, Lane 1 and 2 shows results for normal individuals (III-1 and III-4) while Lane 3, 4, 5 and 6 shows results for affected individuals (III-6, IV-1, IV-2, and IV-3). In the pedigree, Arabic numbers represent the postions of the individuals within a generation and Roman numerals specify the individual's number within the generation.

Sr. No.	Marker ID	Cytogenetic Position (cM)	1	2	3	4	5	6
1.	D17S1828	10.34						
2.	D17S1876	11.48						
3.	D17S1854	13.1						
4.	D17S1832	15.39	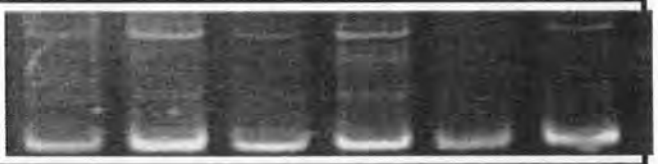					
5.	D17S678	15.65	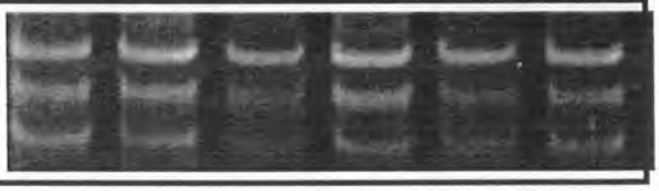					

Figure 3.20: The Electropherogram shows the allelic pattern of family C amplified using microsatellite markers flanking the *NLRP1* gene on chromosome 17q13.2. Here, Lane 1 and 2 shows results for normal individuals (III-1 and III-4) while Lane 3, 4, 5 and 6 shows results for affected individuals (III-6, IV-1, IV-2, and IV-3). In the pedigree, Arabic numbers represent the postions of the individuals within a generation and Roman numerals specify the individual's number within the generation.

Sr. No.	Marker ID	Cytogenetic Position (cM)	1	2	3	4	5	6
1.	D17S902	69.32						
2.	D17S965	69.32	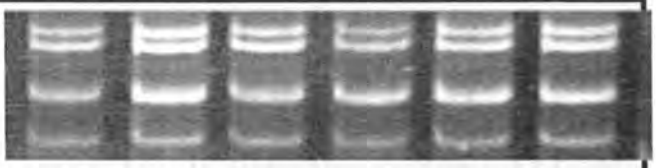					
3.	D17S1860	69.99						
4.	D17S579	69.99	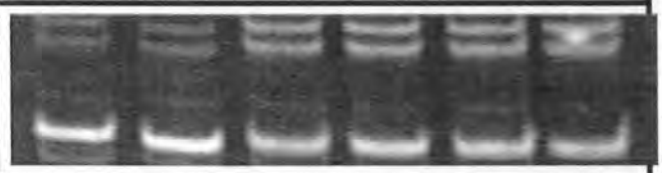					
5.	D17S934	69.99	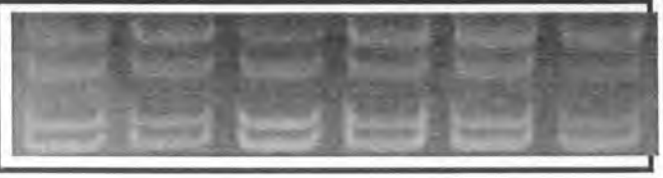					

Figure 3.21: The Electropherogram shows the allelic pattern of family C amplified using microsatellite markers flanking the *JUP* gene on chromosome 17q21.2. Here, Lane 1 and 2 shows results for normal individuals (III-1 and III-4) while Lane 3, 4, 5 and 6 shows results for affected individuals (III-6, IV-1, IV-2, and IV-3). In the pedigree, Arabic numbers represent the postions of the individuals within a generation and Roman numerals specify the individual's number within the generation.

Sr. No.	Marker ID	Cytogenetic Position (cM)	1	2	3	4	5	6
1.	D18S465	91.77	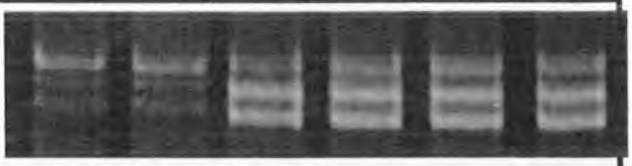					
2.	D18S483	91.77	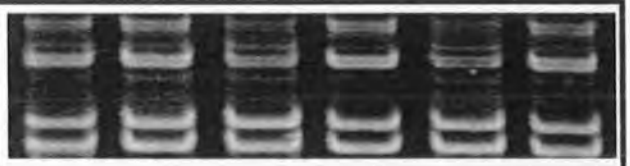					
3.	D18S382	92.61						
4.	D18S875	93.74						
5.	D18S367	93.96	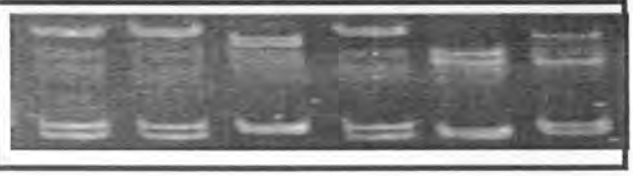					

Figure 3.22: The Electropherogram shows the allelic pattern of family C amplified using microsatellite markers flanking the *SERPINB7* gene on chromosome 18q21.33. Here, Lane 1 and 2 shows results for normal individuals (III-1 and III-4) while Lane 3, 4, 5 and 6 shows results for affected individuals (III-6, IV-1, IV-2, and IV-3). In the pedigree, Arabic numbers represent the postions of the individuals within a generation and Roman numerals specify the individual's number within the generation.

Chapter 4
Discussion

DISCUSSION

Skin and the appendages development, including the hair, nails, teeth, and the sweat glands, is influenced by the genetic control. The defective embryonic developmental mechanisms cause clinically and genetically heterogeneous group of the skin disorders. Further, these disorder are associated to the genotype of the individual either directly or indirectly (Uitto and Richard, 2005; Shah, 2018).

The loss of some or entire hair either on head or the whole body results in a dermatologic disorder called as alopecia. It causes inflammation which in return affects the hair follicles. The phenotypic features associated with the disorder can be mainly skin irritation and loss of eyelashes and eyebrows. Despite being chronic, the disorder is not life threatening, fatal or painful. An autoimmune disorder whose root causes and etiology are yet unknown due to variable manifestations, non-specific presentation and overlapping phenotypes. But majorly both, the genetic and the environmental factors, subsequently are the causes of the development of alopecia (Madani and Shapiro, 2000; Shah, 2018).

Hair is an essential embodiment of the woman identity. Hence the abstract features like attraction, beauty, femininity, sexuality, and personality in general is figuratively linked to women's hair more than it is associated to men hair (Wolf, 1991). Loss of hair is a very common complaint in patients owing to the increased shedding and diffused or localized alopecia (Gordon and Tosti, 2011). The disorder is inherited both in isolated or syndromic forms and is segregated in both the inheritance patterns i.e. autosomal recessive as well as autosomal dominant. So far, eight autosomal recessive and six autosomal dominant forms of non-syndromic forms of hair loss disorders have been reported. The causative genes corresponding to disorders have been successfully mapped on different chromosomes.

Thickening of the stratum corneum on the soles and the palms leads to a diseased condition called palmoplantar keratoderma. Approximately 60 genetically distinct heterogenous group of genodermatosis have been identified so far (Wilson *et al.*, 2010). It is bifurcated on the basis of either acquired or hereditary types. Hereditary types are further divided into diffuse, striate, punctate and focal types (Sakiyama and Kubo,

2016). The pattern of inheritance of PPK can either be autosomal recessive, autosomal dominant, X-linked or mitochondrial inheritance. Keratin filaments, desmosomes, gap junctions and water channels are particularly affected in the PPK diseased condition (Has and Technau-Hafsi, 2016).

An ancient practice of consanguinity, that is associated to genetic abnormities, have a high prevalence in Pakistan due to the lingering societal and spiritual beliefs. For the identification of the genes specifically causing autosomal recessive disorders, the strategy of autozygosity mapping is employed. The method involves the identification of the locus responsible for the diseased phenotypes that is homozygous by decent in the subsequent generations. First cousin marriage with a single affected child is shown to have the exact amount of the linkage information as a nuclear family having three affected individuals (Lander and Botstein, 1987).

The current study conducted the clinical and molecular characterization of three Pakistani families with consanguineous unions (A, B, and C) that presented hereditary skin and hair disorders belonging to rural areas of KPK and Baluchistan province of the country. For this purpose, blood sampling was carried out for DNA extraction. In order to determine the autozygous regions in the families under study, microsatellite markers specific to pre-reported gene/loci were amplified with affected families' extracted DNA.

Family A was identified with non-syndromic form of alopecia with only a single affected individual. Patient exhibited complete hair loss on the scalp as well as other body hair were also absent including eyebrows, eyelashes and beard. Whereas nails, teeth and sweating patterns were unchanged. DNA of the parents and the affected individual were subjected to homozygosity mapping by the help of microsatellite markers flanking the putative genes responsible for autosomal recessive form of alopecia. For genotyping in the main region of the known gene/loci, five markers were selected. The genes tested for linkage analysis included *LIPH* (3q27.2), *HR* (8p21.3), *LPAR6* (13q14.2), and *DSG4/DSC3* (18q12.1). Exclusion of families from known genes was concluded as no linkage was reported upon mapping of gene/loci using highly polymorphic microsatellite markers. The results propose the involvement of novel genes/loci or the corresponding novel variants in these genes causing pathogenicity in family A.

The affected members of family B demonstrated the phenotypes of syndromic form of alopecia with sparse hair on scalp, eyelashes, eyebrows, and beard. The patients particularly showed tightly curled hair termed as Wooly hair. Along with these features, nail discoloration and hypodontia were also seen in affected members. Homozygosity mapping of all the available family memebers was performed by minimum five microsatellite markers for each candidate gene. These genes included *LIPH* (3q27.2), *HR* (8p21.3), *LPAR6* (13q14.2), *CDH3* (16q22.1) and *DSG4/DSC3* (18q12.1). No linkage was established and hence predicting novel genes or the variants responsible for the diseased phenotypes.

Family C presented the clinical features of syndromic form of autosomal recessive palmoplantar keratoderma. The affected members experience skin thickening along with the presence of hyperkeratotic plaques on waxy skin especially palmar and plantar surfaces and also between the digits. Phenotypes including chipped tooth and hammertoes are also displayed by the affected individuals. For autozygosity mapping, minimum five markers were used for genotyping the candidate region of different genes in all available individuals. The genes known to be associated with palmoplantar phenotypes were genotypes and these included *DCAF17* (2q31.1), *SLURP1* (8q24.3), *SDR9C7* (12q13.3), *GJB6* (13q12.11), *NLRP1* (17p13.2), *JUP* (17q21.2), and *SERPINB7* (18q21.33). No evident linkage was observed, therefore, excluding the family from the pre-reported genes and anticipating some novel genes/variants that are suggestive of the pathogenicity in this family.

In family B and C under study, besides the linkage analysis using the polymorphic STS markers, sequencing of two important genes, particularly known to develop the clinical features, i.e. *GJB6* (MIM 604418) and *GJA1*(MIM 604418) was also performed using the Sanger Sequencing. Primer 3 software was used to design primers for both the genes. Diseased individuals in the family B were tested and sequenced for *GJB6* gene that is located on chromosome 13q12.11 and contains only one exon. Family C was checked for the presence of any novel variant existing in the *GJA1* gene, a single exon containing that was mapped on chromosome 6q22.31. To conclude, the dideoxy sequencing results were unable to reveal the involvement of any novel causative gene variant in both the families.

GJB6 (MIM 604418) gene belongs to the connexin superfamily that encodes protein constituents of gap junction channels. They are specifically involved in the transport of ions as well as metabolites across adjacent cells by forming the hexameric hemichannels (Lautermann *et al.*, 1998; Pallares-Ruiz *et al.*, 2002). It encodes a protein connexin 30 (CX30) that comprises 261 amino acids and has a 93% homology with the human *GJB2* protein (Dahl *et al.*, 1996; Grifa *et al.*, 1999). Various missense mutations in the gene lead to a diseased state called Clouston syndrome/ hidrotic ectodermal dysplasia (HED, MIM 129500). It is an autosomal dominant skin disorder that shows the phenotypes of hyperkeratosis leading to palmoplantar, partial to complete hair defects and nail dystrophy (Cammarata *et al.*, 2019). According to HGMD, 28 different mutations have been reported in the *GJB6* gene with 6 particularly associated with HED/Clouston syndrome.

GJA1 (MIM 121014) gene belongs to transmembrane protein family of connexins that interlink two neighboring cells by connecting their cytoplasm via constituting the gap junction proteins (De Bock *et al.*, 2013). It encodes a protein connexin 43 (CX43) that shows 97% homology with the mouse CX43 (Sohl *et al.*, 2003). Perhaps certain mutations in CX43 result in a disease characterized by palmoplantar keratoderma and AP and sometimes nail abnormalities. HGMD reported about 98 various mutations in *GJA1* with much higher incidence of missense mutations (105).

The study aimed at underpinning the molecular basis of the congenital hair loss and ectodermal disorders particularly palmoplantar keratoderma. Furthermore, the study will aid to further provide the future insights into the pathogenesis of above disorders. Over the last two decades, diligent efforts have created an enormous pool of knowledge about the causative genes underlying hair and the skin disorders. But, the identification of the rare phenotypes is quite challenging. In the present era, the focus of the genetic research has been shifted towards the development of the relationship between phenotypes and genotypes. Identification of the genes underlying these rare disorders will eventually lead to the disease cure and developing strategies like gene therapy that will be productive for the disease treatment.

Chapter 5
References

REFERENCES

Ahmad F, Ali RH, Muhammad D, Nasir A, Umair M, Wakil SM, Ramzan K, Basit S, Ahmad W (2016). Novel homozygous sequence variants in the *CDH3* gene encoding P-cadherin underlying hypotrichosis with juvenile macular dystrophy in consanguineous families. Eur J Dermatol 26: 610-612.

Ahmad W, ul Haque MF, Brancolini V, Tsou HC, Ul Haque S, Lam H, Christiano AM (1998). Alopecia universalis associated with a mutation in the human hairless gene. Science 279: 720-724.

Ahmad W, Zlotogorski A, Panteleyev AA, Lam H, Ahmad M, ul Haque MF, Abdallah HM, Dragan L, Christiano AM (1999). Genomic organization of the human hairless gene (HR) and identification of a mutation underlying congenital atrichia in an Arab Palestinian family. Genomics 56: 141-148.

Alazami AM, Al-Saif A, Al-Semari A, Bohlega S, Zlitni S, Alzahrani F, Bavi P, Kaya N, Colak D, Khalak H, Baltus A (2008). Mutations in *C2orf37*, encoding a nucleolar protein, cause hypogonadism, alopecia, diabetes mellitus, mental retardation, and extrapyramidal syndrome. Am J Hum Genet 83: 684-691.

Ali RH, Shah K, Nasir A, Steyaert W, Coucke PJ, Ahmad W (2016). Exome sequencing revealed a novel biallelic deletion in the *DCAF17* gene underlying Woodhouse Sakati syndrome. Clin Genet 90: 263-269.

Alkhalifah, A, Alsantali A, Wang, E, McElwee KJ, Shapiro J (2010). Alopecia areata update: part I. Clinical picture, histopathology, and pathogenesis. J Am Acad Dermatol 62: 177-188.

Alkuraya FS (2010). Homozygosity mapping: one more tool in the clinical geneticist's toolbox. Genet Med 2: 236-239.

Alves R, Grimalt R (2015). Hair loss in children. Alopecias-practical evaluation and management 47: 55-66.

Alves R, Grimalt R (2015). Hair loss in children. Alopecias-practical evaluation and management 47: 55-66.

Aoki J, Inoue A, Makide K, Saiki N, Arai H (2007). Structure and function of extracellular phospholipase A1 belonging to the pancreatic lipase gene family. Biochimie 89: 197-204.

Arkin LM, Ansell L, Rademaker A, Curran ML, Miller ML, Wagner A, Paller AS (2015). The natural history of pediatric-onset discoid lupus erythematosus. J Am Acad Dermatol 72: 628-633.

Aslam M, Chahrour MH, Razzaq A, Haque S, Yan K, Leal SM, Ahmad W (2004). A novel locus for autosomal recessive form of hypotrichosis maps to chromosome 3q26. 33–q27. 3. J Med Genet 41: 849-852

Avashia N, Woolery-Lloyd H, Tosti A, Romanelli P (2010). Short anagen syndrome in an African American woman. *J* Am Acad Dermatol 63: 1092-1093.

Ayub M, Basit, S, Jelani M, Rehman FU, Iqbal M, Yasinzai M, Ahmad W (2009). A homozygous nonsense mutation in the human desmocollin-3 (*DSC3*) gene underlie hereditary hypotrichosis and recurrent skin vesicles. Am J Hum Genet 85: 515-520.

Azeem Z, Jelani M, Naz G, Tariq M, Wasif N, Naqvi SK, Ayub M, Yasinzai M, Wali A, Ali G, Chishti MS (2008). Novel mutations in G protein-coupled receptor gene (P2RY5) in families with autosomal recessive hypotrichosis (LAH3). Hum Genet 123: 515-519

Baran R, de Berker DA, Holzberg M, Thomas L (2012). Baran and Dawber's diseases of the nails and their management. John Wiley & Sons.

Basit S, Ali G, Wasif N, Ansar M, Ahmad W (2010). Genetic mapping of a novel hypotrichosis locus to chromosome 7p21. 3–p22. 3 in a Pakistani family and screening of the candidate genes. Hum Genet 128: 213-220.

Basit S, Khan S, Ahmad W (2015). Genetics of human isolated hereditary hair loss disorders. Clin Genet 88: 203-212.

Basit S, Wali A, Aziz A, Muhammad N, Jelani M, Ahmad W (2011). Digenic inheritance of an autosomal recessive hypotrichosis in two consanguineous pedigrees. Clin Genet 79: 273-281.

Baumer A, Belli S, Trüeb RM, Schinzel A (2000). An autosomal dominant form of hereditary hypotrichosis simplex maps to 18p11. 32–p11. 23 in an Italian family. Eur J Hum Genet 8: 443-448.

Bennett RL, Steinhaus KA, Uhrich SB, O'Sullivan CK, Resta RG, Lochner-Doyle D, Markel DS, Vincent V, Hamanishi J (1995). Recommendations for standardized human pedigree nomenclature. J Genet Couns 4: 267-279.

Betz R C, Lee Y A, Bygum A, Brandrup F, Bernal A I, Toribio J, Alvarez JI, Kukuk GM, Ibsen HHW, Rasmussen HB and Wienker TF, Reis A, Propping P, Kruse R, Cichon S, Nöthen MM (2000). A gene for hypotrichosis simplex of the scalp maps to chromosome 6p21. 3. Am J Hum Genet 66: 1979-1983

Biggs LC, Mikkola ML (2014). Early inductive events in ectodermal appendage morphogenesis. Sem in. Cell Dev Biol 25: 11-21.

Blaydon DC, Lind LK, Plagnol V, Linton KJ, Smith FJ, Wilson NJ, McLean WI, Munro CS, South AP, Leigh IM, O'Toole EA (2013). Mutations in *AQP5*, encoding a water-channel protein, cause autosomal-dominant diffuse non epidermolytic palmoplantar keratoderma. Am J Hum Genet 93: 330-335.

Bouveret E, Rigaut G, Shevchenko A, Wilm M, Séraphin B (2000). A Sm-like protein complex that participates in mRNA degradation. EMBO J 19: 1661-1671

Brauer A (1913). Uber eine besondere Form des hereditaren keratoms (keratoderma disseminatum hereditarium palmare et plantare). Arch Dermatol Syph 114: 211-236.

Braun-Falco M (2009). Hereditary palmoplantar keratodermas. J Dtsch Dermatol Ges 7: 971-984.

Brown FC (1971). Punctate keratoderma. Arch Dermatol 104: 682-683.

Brzezinski P, Pinteala T, Chiriac AE, Foia L, Chiriac A (2015). Aplasia cutis congenita of the scalp-what are the steps to be followed? Case report and review of the literature. Ann Bras Dermatol 90: 100-103.

Buffoli B, Rinaldi F, Labanca M, Sorbellini E, Trink A, Guanziroli E, Rezzani R, Rodella LF (2014). The human hair: from anatomy to physiology. Int J Dermatol 53: 331-341.

Byrne C, Hardman M, Nield K (2003). Covering the limb--formation of the integument. J Anat 202: 113-123.

Cammarata-Scalisi F, Rinelli M, Pisaneschi E, Diociaiuti A, Willoughby CE, Avendaño A, Digilio MC, Novelli A, Callea M (2019). Novel clinical features associated with Clouston syndrome. Int J Dermatol 58: 143-146.

Castelo-Soccio L (2014). Diagnosis and management of alopecia in children. Pediatr Clin 61: 427-442.

Chapalain V, Winter H, Langbein L, Le Roy JM, Labreze C, Nikolic M, Schweizer J, Taïeb A (2002). Is the loose anagen hair syndrome a keratin disorder?: A clinical and molecular study. Arch Dermatol 138: 501-506.

Chen H, Lun Y, Ovchinnikov D, Kokubo H, Oberg KC, Pepicelli CV, Gan L, Lee B, Johnson R (1998). Limb and kidney defects in Lmx1b mutant mice suggest an involvement of *LMX1B* in human nail patella syndrome. Nat Genet 19: 51-55.

Chuong CM, Nickoloff BJ, Elias PM, Goldsmith LA, Macher E, Maderson PA, Sundberg JP, Tagami H, Plonka PM, Thestrup-Pederson K, Bernard BA, Schroder JM, Dotto P, Chang CM, Williams ML, Feingold KR, King LE, Kligman AM, Rees JL, Christophers E (2002). What is the 'true' function of skin? Exp Dermatol 11: 159-187.

Chuong CM, Widelitz RB, Ting-Berreth S, Jiang TX (1996). Early events during avian skin appendage regeneration: dependence on epithelial mesenchymal interaction and order of molecular reappearance. J Invest Dermatol 107: 639-646.

Cichon S, Kruse R, Hillmer AM, Kukuk G, Anker M, Altland K, Knapp M, Propping P, Nöthen MM (2000). A distinct gene close to the hairless locus on chromosome 8p underlies hereditary Marie Unna type hypotrichosis in a German family. Br J Dermatol 143: 811-814.

Clark RA (1985). Cutaneous tissue repair: basic biologic considerations. I. J Am Acad Dermatol 13: 701-725.

Clissold PM, Ponting CP (2001). JmjC: cupin metalloenzyme-like domains in jumonji, hairless and phospholipase A2β. Trends Biochem Sci 26: 7-9.

Cotter L, Cheng K, Kirkorian AY (2017). Anagen effluvium in association with extracorporeal membrane oxygenation. Pediatr Dermatol 34: e201-202.

Cutrone M, Grimalt R (2005). Transient neonatal hair loss: a common transient neonatal dermatosis. Eur J Pediatr164: 630-632.

Dahl E, Manthey D, Chen Y, Schwarz HJ, Chang YS, Lalley PA, Nicholson BJ, Willecke K (1996). Molecular cloning and functional expression of mouse connexin-30, a gap junction gene highly expressed in adult brain and skin. J Biol Chem 271:17903-17910.

De Bock M, Kerrebrouck M, Wang N, Leybaert L (2013). Neurological manifestations of oculodentodigital dysplasia: a Cx43 channelopathy of the central nervous system?. Front Pharmacol 4: 120.

Dhurat RP, Deshpande DJ (2010). Loose anagen hair syndrome. Int J Trichology 2: 96.

Djabali K, Aita VM, Christiano AM (2001). Hairless is translocated to the nucleus via a novel bipartite nuclear localization signal and is associated with the nuclear matrix. J Cell Sci 114: 367-376.

Djabali K, Christiano AM (2004). Hairless contains a novel nuclear matrix targeting signal and associates with histone deacetylase 3 in nuclear speckles. Differentiation. 72: 410-418.

Dreyer SD, Zhou G, Baldini A, Winterpacht A, Zabel B, Cole W, Johnson RL, Lee B (1998). Mutations in *LMX1B* cause abnormal skeletal patterning and renal dysplasia in nail patella syndrome. Nat Genet 19: 47-50.

Durmowicz MC, Cui CY, Schlessinger D (2002). The EDA gene is a target of, but does not regulate Wnt signaling. Gene 285: 203-211.

Duverger O, Morasso MI (2014). To grow or not to grow: hair morphogenesis and human genetic hair disorders. Sem in Cell Dev 25: 22-33.

Eliason MJ, Leachman SA, Feng BJ, Schwartz ME, Hansen CD (2012). A review of the clinical phenotype of 254 patients with genetically confirmed pachyonychia congenita. J Am Acad Dermatol 67: 680-686.

Erdoğan, B. (2017). Anatomy and physiology of hair. Hair and Scalp Disorders. 13.

Fischer J, Bouadjar B, Heilig R, Huber M, Lefèvre C, Jobard F, Lathrop M (2001). Mutations in the gene encoding SLURP-1 in Mal de Meleda. Hum Mol Genet 10: 875-880.

Fremerey C, Nenoff P (2018). Tinea capitis in a newborn. N Engl J Med 378: 2021-2022

Gach JE, Munro CS, Lane EB, Wilson NJ, Moss C (2005). Two families with Greither's syndrome caused by a keratin 1 mutation. *J.* Am. Acad. Dermatol 53: S225-S230.

García-Martín P, Hernández-Martín A, Torrelo A (2013). Ectodermal dysplasias: a clinical and molecular review. Actas Dermo-Sifiliográficas (English Edition). 104: 451-470.

Garrod D, Chidgey M (2008). Desmosome structure, composition and function. Biochim Biophys Acta Biomembr 1778: 572-587.

Giacomini F, Starace M, Tosti A. Short anagen syndrome (2011). Pediatr Dermatol 28: 133-134.

Giehl KA, Eckstein GN, Pasternack SM, Praetzel-Wunder S, Ruzicka T, Lichtner P, Seidl K, Rogers M, Graf E, Langbein L, Braun-Falco M (2012). Nonsense

mutations in *AAGAB* cause punctate palmoplantar keratoderma type Buschke-Fischer-Brauer. Am J Hum Genet 91: 754-759.

Gonzalez ME, Cantatore-Francis J, Orlow SJ (2010). Androgenetic alopecia in the paediatric population: a retrospective review of 57 patients. Br J Dermatol 163: 378-385.

Gordon KA, Tosti A (2011). Alopecia: evaluation and treatment. Clin Cosmet Investig Dermatol. 4:101.

Grant JE, Chamberlain SR (2016). Trichotillomania. Am J Psychiatry 173: 868-874.

Grifa A, Wagner CA, D'Ambrosio L, Melchionda S, Bernardi F, Lopez-Bigas N, Rabionet R, Arbones M, Della Monica M, Estivill X, Zelante L (1999). Mutations in GJB6 cause nonsyndromic autosomal dominant deafness at DFNA3 locus. Nat Genet 23: 16-18.

Guo BR, Zhang X, Chen G, Zhang JG, Sun LD, Du WD, Zhang Q, Cui Y, Zhu J, Tang XF, Xiao R (2012). Exome sequencing identifies a *COL14A1* mutation in a large Chinese pedigree with punctate palmoplantar keratoderma. Am J Med Genet 49: 563-568.

Harrison S, Sinclair R (2003). Hair colouring, permanent styling and hair structure. J Cosmet Dermatol 2: 180-185.

Has C, Technau-Hafsi K (2016). Palmoplantar keratodermas: clinical and genetic aspects. J Dtsch Dermatol Ges 14: 123-140.

He PP, Zhang XJ, Yang Q, Li M, Liang YH, Yang S, Huang W (2004). Refinement of a locus for Marie Unna hereditary hypotrichosis to a 1· 1-cM interval at 8p21. 3. Br J Dermatol 150: 837-842

He Y, Zeng K, Zhang X, Chen Q, Wu J, Li H, Zhou Y, Glusman G, Roach J, Etheridge A, Qing S (2015). A gain-of-function mutation in *TRPV3* causes focal palmoplantar keratoderma in a Chinese family. J Invest Dermatol 135: 907-909.

Headington JT (1993). Telogen effluvium: new concepts and review. Arch Dermatol 129: 356-363.

Herskovitz I, de Sousa ICVD, Simon J, Tosti A (2013). Short anagen hair syndrome. Int J Trichol 5: 45.

Holm SJ, Carlen LM, Mallbris L, Ståhle-Bäckdahl M, O'Brien KP (2003). Polymorphisms in the SEEK1 and SPR1 genes on 6p21. 3 associate with psoriasis in the Swedish population. Exp Dermatol 12: 435-444.

Hu JC, Simmer JP (2007). Developmental biology and genetics of dental malformations. Orthod Craniofac Res 10: 45-52.

Huang S, Zhu X, Liu Y, Tao Y, Feng G, He L, Guo X, Ma G (2012). Wls is expressed in the epidermis and regulates embryonic hair follicle induction in mice.

Itin PH (2014). Etiology and pathogenesis of ectodermal dysplasias. Am J Med Genet 164: 2472-2477.

Ito S, Wakamatsu K (2011). Human hair melanins: what we have learned and have not learned from mouse coat color pigmentation. Pigment Cell Melanoma Res 24: 63-74.

Jelani M, Salman CM, Ahmad W (2009). A novel splice-site mutation in the CDH3 gene in hypotrichosis with juvenile macular dystrophy. Clin Exp Dermatol: Clin Dermatol 34: 68-73.

Jelani M, Wasif N, Ali G, Chishti MS, Ahmad W (2008). A novel deletion mutation in LIPH gene causes autosomal recessive hypotrichosis (LAH2). Clin Genet 74: 184-188.

John P, Ali G, Chishti MS, Naqvi SM, Leal SM, Ahmad W (2006). Localization of a novel locus for alopecia with mental retardation syndrome to chromosome 3q26. 33–q27. 3. Hum Genet 118: 665-667.

Jumlongras D, Bei M, Stimson JM, Wang WF, DePalma SR, Seidman CE, Felbor U, Maas R, Seidman JG, Olsen BR (2001). A nonsense mutation in *MSX1* causes Witkop syndrome. Am J Hum Genet 69: 67-74.

Kabashima K, Sakabe JI, Yamada Y, Tokura Y (2008). "Nagashima-type" keratosis as a novel entity in the palmoplantar keratoderma category. Arch dermatol 144: 375-379.

Kanwar AJ, Narang T (2013). Anagen effluvium. Indian J Dermatol Venereol Leprol 79: 604.

Kastl I, Anton-Lamprecht I, Gamborg Nielsen P (1990). Hereditary palmoplantar keratosis of the Gamborg-Nielsen type. Clinical and ultrastructural characteristics of a new type of autosomal recessive palmoplantar keratosis. Arch Dermatol Res 282: 363-370.

Kersey PJ. Tricho-dental syndrome: a disorder with a short hair cycle (1987). Br J Dermatol 116: 259-263.

Kibar M, Aktan Ş, Bilgin M (2014). Scalp dermatoscopic findings in androgenetic alopecia and their relations with disease severity. Ann Dermatol 26: 478.

Kim MS, Na CH, Choi H, Shin BS (2011). Prevalence and factors associated with neonatal occipital alopecia: a retrospective study. Ann Dermatol 23: 288.

Kjaer KW, Hansen L, Schwabe GC, Marques-de-Faria AP, Eiberg H, Mundlos S, Tommerup N, Rosenberg T (2005). Distinct *CDH3* mutations cause ectodermal dysplasia, ectrodactyly, macular dystrophy (EEM syndrome). J Med Genet 42: 292-298.

Knöbel M, O'Toole EA, Smith FJ (2015). Keratins and skin disease. Cell Tissue Res 360: 583-589.

Kruse R, Cichon S, Anker M, Hillmer AM, Barros-Núñez P, Cantú JM, Leal E, Weinlich G, Schmuth M, Fritsch P, Ruzicka T (1999). Novel hairless mutations in two kindreds with autosomal recessive papular atrichia. J Invest Dermatol 113: 954-959.

Kubo A, Oura Y, Hirano T, Aoyama Y, Sato S, Nakamura K, Takae Y, Amagai M (2013). Collapse of the keratin filament network through the expression of mutant keratin 6c observed in a case of focal plantar keratoderma. J Dermatol 40: 553-557.

Kubo A, Shiohama A, Sasaki T, Nakabayashi K, Kawasaki H, Atsugi T, Sato S, Shimizu A, Mikami S, Tanizaki H, Uchiyama M (2013). Mutations in *SERPINB7*, encoding a member of the serine protease inhibitor superfamily, cause Nagashima-type palmoplantar keratosis. Am J Hum Genet 93: 945-956.

Kunisada M, Cui CY, Piao Y, Ko MS, Schlessinger D (2009). Requirement for Shh and Fox family genes at different stages in sweat gland development. Hum Mol Genet 18: 1769-1778.

Küster W, Reis A, Hennies H (2002). Epidermolytic palmoplantar keratoderma of Vorner: re-evaluation of Vorner's original family and identification of a novel keratin 9 mutation. Arch Dermatol Res 294: 268-272.

Lai-Cheong JE, McGrath JA (2013). Structure and function of skin, hair and nails. Medicine 41: 317-320.

Lai-Cheong JE, McGrath JA (2017). Structure and function of skin, hair and nails. Medicine 45: 347-351.

Lander ES, Botstein D (1987). Homozygosity mapping: a way to map human recessive traits with the DNA of inbred children. Science 236: 1567-1570.

Laurikkala J, Pispa J, Jung HS, Nieminen P, Mikkola M, Wang X, Saarialh o-Kere U, Galceran J, Grosschedl R, Thesleff I (2002). Regulation of hair follicle development by the TNF signal ectodysplasin and its receptor Edar. Development 129: 2541-2553.

Lautermann J, Wouter-Jan F, Altenhoff P, Grümmer R, Traub O, Frank HG, Jahnke K, Winterhager E (1998). Expression of the gap-junction connexins 26 and 30 in the rat cochlea. Cell Tissue Res 294: 415-420.

Lefevre P, Rochat A, Bodemer C, Vabres P, Barrandon Y, de Prost Y, Garner C, Hovnanian A (2000). Linkage of Marie-Unna hypotrichosis locus to chromosome

8p21 and exclusion of 10 genes including the hairless gene by mutation analysis. Eur J Hum Genet 8: 273-279.

Lewin AB, Piacentini J, Flessner CA, Woods DW, Franklin ME, Keuthen NJ, Stein DJ (2009). Depression, anxiety, and functional impairment in children with trichotillomania. Depression and Anxiety 26: 521-527.

Li VCY, Yesudian PD (2015). Congenital triangular alopecia. Int J trichology 7: 48.

Lind L, Lundstrom A, Hofer PA, Holmgren G (1994). The gene for diffuse palmoplantar keratoderma of the type found in northern Sweden is localized to chromosome 12q11-q13. Hum Mol Genet 3: 1789-1793.

Loewenthal LJA, Prakken JR (1961). Atrichia with popular lesions. Dermatology 122: 85-89.

Loomis CA, Harris E, Michaud J, Wurst W, Hanks M, Joyner AL (1996). The mouse Engrailed-1 gene and ventral limb patterning. Nature 382: 360-363.

Madani S, Shapiro J (2000). Alopecia areata update. J Am Acad Dermatol: 42: 549-66.

Marneros AG (2013). BMS1 is mutated in aplasia cutis congenita. PLoS Genet 9: e1003573.

Marneros AG (2015).Genetics of aplasia cutis reveal novel regulators of skin morphogenesis. J Invest Dermatol 135: 666-672.

Matise TC, Chen F, Chen W, Francisco M, Hansen M, He C, Hyland FC, Kennedy GC, Kong X, Murray SS, Ziegle JS (2007). A second-generation combined linkage–physical map of the human genome. Genome Res 17:1783-1786.

McKittrick J, Chen PY, Bodde SG, Yang W, Novitskaya EE, Meyers MA (2012). The structure, functions, and mechanical properties of keratin. Jom 64: 449-468.

Migeon BR, Brown TR, Axelman J, Migeon CJ (1981). Studies of the locus for androgen receptor: localization on the human X chromosome and evidence for homology with the Tfm locus in the mouse. Proc Natl Acad Sci 78: 6339-6343.

Mikkola ML (2007). Genetic basis of skin appendage development. Sem in Cell Dev Biol 18: 225-236.

Mirmirani P, Khumalo NP (2014). Traction alopecia: How to translate study data for public education—closing the KAP gap?. Dermatol Clin 32: 153-161.

Mou C, Jackson B, Schneider P, Overbeek PA, Headon DJ (2006). Generation of the primary hair follicle pattern. Proc Natl Acad Sci 103: 9075-9080.

Nagashima M (1977). Molecular genetic studies in families with the Conradi-Hunermann-Happle palmoplantar keratoses. In handbook of human genetics, Volume 9. Tokyo: Igaku Shoin.

Naz G, Ali G, Naqvi SK, Azeem Z, Ahmad, W (2010). Mapping of a novel autosomal recessive hypotrichosis locus on chromosome 10q11. 23–22.3. Hum Genet 127: 395-401.

Nöthen MM, Cichon S, Vogt IR, Hemmer S, Kruse R, Knapp M, Höller T, ul Haque MF, Haque S, Propping P, Ahmad M (1998). A gene for universal congenital alopecia maps to chromosome 8p21-22. Am J Hum Genet 62: 386-390.

Olabiyi AO, Akpantah AO, Oyerinde FO, Gbotolorun SC, Eluwa MA, Ekanem TB (2008). The distribution of hair on the phalanges of a sample population of Nigerian Yorubas in relation to sex, age and job type. Niger J Physiol Sci 23

Onoufriadis AL, Cabezas A, Ng JC, Canales J, Costas MJ, Ribeiro JM, Rodrigues JR, McAleer MA, Castelo-Soccio L, Simpson MA, Fraternali F (2020). Autosomal recessive hypotrichosis with loose anagen hairs associated with TKFC mutations. Br J Dermatol

Pagnan NAB, Visinoni AF (2014). Update on ectodermal dysplasias clinical classification. Am J Med Genet A 164: 2415-2423.

Pallares-Ruiz N, Blanchet P, Mondain M, Claustres M, Roux AF (2002). A large deletion including most of GJB6 in recessive non syndromic deafness: a digenic effect?. Eur J Hum Genet 10: 72-76.

Pasternack SM, Murugusundram S, Eigelshoven S, Müller M, Kruse R, Lehmann P, Betz RC (2009). Novel mutations in the P2RY5 gene in one Turkish and two Indian patients presenting with hypotrichosis and woolly hair. Arch Dermatol Res 301: 621-624.

Pasternack SM, Refke M, Paknia E, Hennies HC, Franz T, Schäfer N, Betz RC (2013). Mutations in *SNRPE*, which encodes a core protein of the spliceosome, cause autosomal-dominant hypotrichosis simplex. Am J Hum Genet 92: 81-87.

Patel S, Zirwas M, English JC (2007). Acquired palmoplantar keratoderma. Am J Clin Dermatol 8: 1-11.

Popescu NC, Bowden PE, DiPaolo JA (1989). Two type II keratin genes are localized on human chromosome 12. Hum Genet 82: 109-112.

Priolo M (2009). Ectodermal dysplasias: an overview and update of clinical and molecular-functional mechanism. Am J Med Genet A 149: 2003-2013.

Pummila M, Fliniaux I, Jaatinen R, James MJ, Laurikkala J, Schneider P, Thesleff I, Mikkola ML (2007). Ectodysplasin has a dual role in ectodermal organogenesis: inhibition of Bmp activity and induction of Shh expression. Development 134: 117-125.

Qi J, Garza LA (2014). An overview of alopecias. Cold Spring Harb Perspect Med 4: a013615.

Randall VA, Botchkareva NV (2009). Cosmetic applications of laser and light-based systems. 3-35.

Reis A, Hennies HC, Langbein L, Digweed M, Mischke D, Drechsler M, Küster W (1994). *Keratin 9* gene mutations in epidermolytic palmoplantar keratoderma (EPPK). Nat Genet 6: 174-179.

Rishikaysh P, Dev K, Diaz D, Qureshi WMS, Filip S, Mokry J (2014). Signaling involved in hair follicle morphogenesis and development. Int J Mol Sci 15: 1647-1670.

Rishikaysh P, Dev K, Diaz D, Qureshi WMS, Filip S, Mokry J (2014). Signaling involved in hair follicle morphogenesis and development. Int J Mol Sci 15: 1647-1670.

Rodríguez-García C, González-Hernández S, Hernández-Martín A, Pérez- Robayna N, Sanchez R, Torrelo A (2011). Aplasia cutis congenita and other anomalies associated with methimazole exposure during pregnancy. Pediatr Dermatol 28: 743-745.

Ross FP, Christiano AM (2006). Nothing but skin and bone. J Clin Invest 116: 1140-1149.

Safavi K (1992). Prevalence of alopecia areata in the first national health and nutrition examination survey. Arch Dermatol 128: 702-702

Sakiyama T, Kubo A (2016). Hereditary palmoplantar keratoderma "clinical and genetic differential diagnosis". J Dermatol 43: 264-274.

Sakiyama T, Kubo A (2016). Hereditary palmoplantar keratoderma "clinical and genetic differential diagnosis". Int J Dermatol 43: 264-274.

Salgado-Garrido J, Bragado-Nilsson E, Kandels-Lewis S, Séraphin B (1999). Sm and Sm-like proteins assemble in two related complexes of deep evolutionary origin. EMBO J 18: 3451-3462.

Sambrook J, Fritsch EF, Maniatis (1989). Molecular cloning: A laboratory manual, 2nd edition, Cold Spring Laboratory Press.

Sartaj R, Sharpe P (2006). Biological tooth replacement. J Anat 209: 503-509.

Schiller S, Seebode C, Hennies HC, Giehl K, Emmert S (2014). Palmoplantar keratoderma (PPK): acquired and genetic causes of a not so rare disease. J Dtsch Dermatol Ges 12: 781-788.

Segre JA (2006). Epidermal barrier formation and recovery in skin disorders. J Clin Invest 116: 1150-1158.

Séraphin B (1995). Sm and Sm-like proteins belong to a large family: identification of proteins of the U6 as well as the U1, U2, U4 and U5 snRNPs. EMBO J 14: 2089-2098.

Shah K (2018). Mapping genes causing syndromic and non-syndromic human hereditary skin disorders (Doctoral dissertation, Quaid-i-Azam University Islamabad).

Shimomura Y (2012). Congenital hair loss disorders: rare, but not too rare. J Dermatol 39: 3-10.

Shimomura Y, Agalliu D, Vonica A, Luria V, Wajid M, Baumer A, Belli S, Petukhova L, Schinzel A, Brivanlou AH, Barres BA (2010). APCDD1 is a novel Wnt inhibitor mutated in hereditary hypotrichosis simplex. Nature 464: 1043-1047.

Shimomura Y, Christiano AM (2010). Biology and genetics of hair. Ann Rev Genomics Hum Genet 11: 109-32.

Shimomura Y, Wajid M, Ishii Y, Shapiro L, Petukhova L, Gordon D, Christiano AM (2008). Disruption of P2RY5, an orphan G protein–coupled receptor, underlies autosomal recessive woolly hair. Nat Genet 40: 335-339.

Shimomura Y, Wajid M, Petukhova L, Kurban M, Christiano AM (2010). Autosomal-dominant woolly hair resulting from disruption of keratin 74 (*KRT74*), a potential determinant of human hair texture. Am J Human Genet 86: 632-638.

Shimomura Y, Wajid M, Petukhova L, Shapiro L, Christiano AM (2009). Mutations in the lipase H gene underlie autosomal recessive woolly hair/hypotrichosis. J Invest Dermatol 129: 622-628.

Simon M, Jonca N, Guerrin M, Haftek M, Bernard D, Caubet C, Egelrud T, Schmidt R, Serre G (2001). Refined characterization of corneodesmosin proteolysis during terminal differentiation of human epidermis and its relationship to desquamation. J Biol Chem 276: 20292-20299.

Söhl G, Nielsen PA, Eiberger J, Willecke K (2003). Expression profiles of the novel human connexin genes hCx30. 2, hCx40. 1, and hCx62 differ from their putative mouse orthologues. Cell Commun Adhes 10: 27-36.

Sonoda H, Aoki J, Hiramatsu T, Ishida M, Bandoh K, Nagai Y, Taguchi R, Inoue K, Arai H (2002). A novel phosphatidic acid-selective phospholipase A1that produces lysophosphatidic acid. J Biol Chem 277: 34254-34263.

Spano F, Donovan JC (2015). Alopecia areata: Part 1: pathogenesis, diagnosis and prognosis. Canad Fam Phys 61: 751-755.

Sprecher E, Bergman R, Richard G, Lurie R, Shalev S, Petronius D, Shalata A, Anbinder Y, Leibu R, Perlman I, Cohen N, Szargel R (2001). Hypotrichosis with juvenile macular dystrophy is caused by a mutation in *CDH3*, encoding P-cadherin. Nat Genet 29: 134-136.

Sreekumar GP, Roberts JL, Wong CQ, Stenn KS, Parimoo S (2000). Marie Unna hereditary hypotrichosis gene maps to human chromosome 8p21 near hairless. J Invest Dermatol 114: 595-597.

Swink SM, Castelo-Soccio L (2016). Loose anagen syndrome: a retrospective chart review of 37 cases. Pediatr Dermatol 33: 507-510.

Sybert VP, Dale BA, Holbrook KA (1988). Palmar-plantar keratoderma: a clinical, ultrastructural, and biochemical study. J Am Acad Dermatol 18: 75-86.

Tariq M, Ayub M, Jelani M, Basit S, Naz G, Wasif N, Raza SI, Naveed AK, Ullah KS, Azeem Z, Yasinzai M (2009). Mutations in the P2RY5 gene underlie autosomal recessive hypotrichosis in 13 Pakistani families. Br J Dermatol 160: 1006-1010.

Tocchetti A, Confalonieri S, Scita G, Di Fiore PP, Betsholtz C (2003). In silico analysis of the EPS8 gene family: genomic organization, expression profile, and protein structure. Genomics 81: 234-244.

Tosti A, Misciali C, Borrello P, Fanti PA, Bardazzi F, Patrizi A (1991). Loose anagen hair in a child with Noonan's syndrome. Dermatology 182: 247-249.

Tucker A, Sharpe P (2004). The cutting-edge of mammalian development; how the embryo makes teeth. Nat Rev Genet 5: 499-508.

Uitto J, Richard G (2005). Progress in epidermolysis bullosa: from eponyms to molecular genetic classification. Clin Dermatol 23: 33-40

Ullah A, Raza SI, Ali RH, Naveed AK, Jan A, Rizvi SD, Satti R, Ahmad W (2015). A novel deletion mutation in the DSG4 gene underlies autosomal recessive hypotrichosis with variable phenotype in two unrelated consanguineous families. Clin Exp Dermatol 40: 78-84.

van Steensel M, Smith FJ, Steijlen PM, Kluijt I, Stevens HP, Messenger A, Kremer H, Dunnill MG, Kennedy C, Munro CS, Doherty VR (1999). The gene for hypotrichosis of Marie Unna maps between D8S258 and D8S298: exclusion of the hr gene by cDNA and genomic sequencing. Am J Hum Genet 65: 413-419.

Wajid M, Bazzi H, Rockey J, Lubetkin J, Zlotogorski A, Christiano AM (2007). Localized autosomal recessive hypotrichosis due to a frameshift mutation in the desmoglein 4 gene exhibits extensive phenotypic variability within a Pakistani family. J Invest Dermatol 127: 1779-1782.

Wali A, Ali G, John P, Lee K, Chishti MS, Leal SM, Ahmad W (2007). Mapping of a gene for alopecia with mental retardation syndrome (APMR3) on chromosome 18q11.2-q12.2. Ann Hum Genet 71: 570-577.

Wali A, Chishti MS, Ayub M, Yasinzai M, Kafaitullah, Ali G, John P, Ahmad W (2007). Localization of a novel autosomal recessive hypotrichosis locus (LAH3) to chromosome 13q14. 11–q21. 32. Clin Genet 72: 23-29.

Wali A, John P, Gul A, Lee K, Chishti MS, Ali G, Hassan MJ, Leal SM, Ahmad W (2006). A novel locus for alopecia with mental retardation syndrome (APMR2) maps to chromosome 3q26.2-q26.31. Clin Genet 70: 233-239.

Wasif N, Basit S, Ali N, Ansar M, Ahmad W (2011). Novel mutations in the keratin-74 (*KRT74*) gene underlie autosomal dominant woolly hair/hypotrichosis in Pakistani families. Human Genet 129: 419-424.

Welle MM, Wiener DJ (2016). The hair follicle: a comparative review of canine hair follicle anatomy and physiology. Toxicol Pathol 44: 564-574.

Wen Y, Liu Y, Xu Y, Zhao Y, Hua R, Wang K, Zhang, X (2009). Loss- of-function mutations of an inhibitory upstream ORF in the human hairless transcript cause Marie Unna hereditary hypotrichosis. Nature Genet 41: 228-233.

Whittock NV, Ashton GH, Dopping HPJ, Gratian MJ, Keane FM, Eady RA, McGrath JA (1999). Striate palmoplantar keratoderma resulting from desmoplakin haploinsufficiency. J Invest Dermatol 113: 940-946.

Whittock NV, Smith FJ, McLean WI, Wan H, Mallipeddi R, Griffiths WA, Dopping Hepenstal P, Ashton GH, Eady RA, McGrath JA (2002). Frameshift mutation in the V2 domain of human keratin 1 results in striate palmoplantar keratoderma. J Invest Dermatol 118: 838-844.

Wilson NJ, Messenger AG, Leachman SA, O'Toole EA, Lane EB, McLean WI, Smith FJ (2010). Keratin K6c mutations cause focal palmoplantar keratoderma. J Invest Dermatol 130: 425-429.

Wilson NJ, Messenger AG, Leachman SA, O'Toole EA, Lane EB, McLean WI, Smith FJ (2010). Keratin K6c mutations cause focal palmoplantar keratoderma. J Invest Dermatol 130: 425-429.

Wolf N (1991). The beauty myth. New York

Wolff H, Fischer TW, Blume-Peytavi U (2016). The diagnosis and treatment of hair and scalp diseases. Dtsch Ärztebl Int 113: 377.

Xu C, Zhang L, Chen N, Su B, Pan CM, Li JY, Song, H. D (2010). A new locus for hereditary hypotrichosis simplex maps to chromosome 13q12. 12~ 12.3 in a Chinese family. J Cutan Patho 37: 758-763.

Xu L, Liu KX, Senna MM (2017). A practical approach to the diagnosis and management of hair loss in children and adolescents. Front Med 4: 112.

Yan KL, He PP, Yang S, Li M, Yang Q, Ren YQ, Zhang XJ (2004). Marie Unna hereditary hypotrichosis: report of a Chinese family and evidence for genetic heterogeneity. Clin Exp Dermatol: Clin Dermatol 29: 460-463

Yang CC, Cotsarelis G (2010). Review of hair follicle dermal cells. J Dermatol Sci 57: 2-11.

Yoshihama M, Uechi T, Asakawa S, Kawasaki K, Kato S, Higa S, Maeda N, Minoshima S, Tanaka T, Shimizu N, Kenmochi N (2002). The human ribosomal protein genes: sequencing and comparative analysis of 73 genes. Genome Res 12: 379-390.

Yu Y, Yang W, Wang, B, Meyers MA (2017). Structure and mechanical behavior of human hair. Mater Sci Eng C 73: 152-163.

Zaraa I, Hawilo A, Aounallah A, Trojjet S, El ED, Mokni M, Osman AB (2013). Inflammatory Tinea capitis: a 12-year study and a review of the literature. Mycoses 56: 110-116.

Zhang X, Guo BR, Cai LQ, Jiang T, Sun LD, Cui Y, Zhang XJ (2012). Exome sequencing identified a missense mutation of EPS8L3 in Marie Unna hereditary hypotrichosis. J Med Genet 49: 727-730.

Zhao L, Vahlquist A, Virtanen M, Wennerstrand L, Lind LK, Lundström A, Pigg MH (2014). Palmoplantar keratoderma of the Gamborg-Nielsen type is caused by mutations in the SLURP1 gene and represents a variant of Mal de Meleda. Acta Dermato-Venereologica. 94: 707-710.

Zhou C, Zang D, Jin Y, Wu H, Liu Z, Du J, Zhang J (2011). Mutation in ribosomal protein L21 underlies hereditary hypotrichosis simplex. Hum Mutat 32: 710-714.

Zlotogorski A, Martinez-Mir A, Green J, Lam H, Panteleyev AA, Sinclair R, Christiano AM (2002a). Evidence for pseudodominant inheritance of atrichia with papular lesions. J Invest Dermatol 118: 881-886.

Zlotogorski A, Panteleyev AA, Aita VM, Christiano AM (2002b). Clinical and molecular diagnostic criteria of congenital atrichia with papular lesions. J Invest Dermatol 118: 887-890.

Clinical and Genetic Analysis of Alopecia and Ectodermal Dysplasia in Three Consanguineous Families

by Kamran Saeed

inical and Genetic Analysis of Alopecia and Ectodermal ysplasia in Three Consanguineous Families

GINALITY REPORT

7 %	4%	4%	3%
MILARITY INDEX	INTERNET SOURCES	PUBLICATIONS	STUDENT PAPERS

MARY SOURCES

1	Submitted to Higher Education Commission Pakistan Student Paper	2%
2	onlinelibrary.wiley.com Internet Source	1%
3	prr.hec.gov.pk Internet Source	1%
4	jamanetwork.com Internet Source	1%
5	ijcmas.com Internet Source	<1%
6	Submitted to The University of Manchester Student Paper	<1%
7	Basit, S., S. Khan, and W. Ahmad. "Genetics of human isolated hereditary hair loss disorders : Genetics of hereditary hair loss disorders", Clinical Genetics, 2014. Publication	<1%